Inter-ocular contrast normalization in human visual cortex

Farshad Moradi   Department of Psychology and Center for Neural Science, New York University, New York, NY, USA

David J. Heeger   Department of Psychology and Center for Neural Science, New York University, New York, NY, USA

The brain combines visual information from the two eyes and forms a coherent percept, even when inputs to the eyes are different. However, it is not clear how inputs from the two eyes are combined in visual cortex. We measured fMRI responses to single gratings presented monocularly, or pairs of gratings presented monocularly or dichoptically with several combinations of contrasts. Gratings had either the same orientation or orthogonal orientations (i.e., plaids). Observers performed a demanding task at fixation to minimize top-down modulation of the stimulus-evoked responses. Dichoptic presentation of compatible gratings (same orientation) evoked greater activity than monocular presentation of a single grating only when contrast was low (<10%). A model that assumes linear summation of activity from each eye failed to explain binocular responses at 10% contrast or higher. However, a model with binocular contrast normalization, such that activity from each eye reduced the gain for the other eye, fitted the results very well. Dichoptic presentation of orthogonal gratings evoked greater activity than monocular presentation of a single grating for all contrasts. However, activity evoked by dichoptic plaids was equal to that evoked by monocular plaids. Introducing an onset asynchrony (stimulating one eye 500 ms before the other, which under attentive vision results in flash suppression) had no impact on the results; the responses to dichoptic and monocular plaids were again equal. We conclude that when attention is diverted, inter-ocular suppression in V1 can be explained by a normalization model in which the mutual suppression between orthogonal orientations does not depend on the eye of origin, nor on the onset times, and cross-orientation suppression is weaker than inter-ocular (same orientation) suppression.

Keywords: binocular vision, suppression, primary visual cortex, V1, functional magnetic resonance imaging, fMRI

Citation: Moradi, F., & Heeger, D. J. (2009). Inter-ocular contrast normalization in human visual cortex. *Journal of Vision,* *9*(3):13, 1–22, http://journalofvision.org/9/3/13/, doi:10.1167/9.3.13.

Introduction

Doubling of the input to the visual cortex in binocular vs. monocular viewing hardly results in a noticeable difference in our subjective perceptual experience. Only at low contrasts and/or for brief stimulus presentations does binocular stimulation affect psychophysical performance: visual acuity (Cagenello, Arditi, & Halpern, 1993; Zlatkova, Anderson, & Ennis, 2001), contrast sensitivity (Legge, 1984), orientation discrimination (Bearse & Freeman, 1994), or perceived contrast (Baker, Meese, & Georgeson, 2007). These effects are negligible at higher contrasts.

Pre-cortical pathways in the retina and lateral geniculate nucleus (LGN) are separate and independent for stimuli presented to the two eyes, such that any interaction between inputs from the two eyes must primarily reflect cortical mechanisms. Stimulating two eyes instead of one should theoretically double the LGN input to primary visual cortex (V1), and therefore, if unopposed, should increase the overall neural activity in V1 in two ways. First, compared to monocular stimulation, twice the number of monocular neurons (i.e., neurons that receive inputs exclusively from one eye) are activated by binocular stimulation. Second, binocular neurons receive double the excitatory synaptic input from LGN axons. Without a suppressive mechanism for balancing this larger excitatory drive, or other regulatory mechanisms, binocular stimuli would evoke considerably more synaptic and neural activity than monocular stimuli; that should be evident using any of a number of measures of population activity including functional magnetic resonance imaging (fMRI).

The response of a visual neuron to a preferred stimulus can be suppressed by the simultaneous presentation of other stimuli. There is an extensive literature on such suppressive phenomena in V1 (for a review of the early literature, see Heeger, 1992a, 1992b). For example, the responses of a V1 neuron to an optimally oriented stimulus are diminished by superimposing an orthogonal stimulus that is ineffective in driving the cell when presented alone (Bauman & Bonds, 1991; Bonds, 1989; Carandini, Heeger, & Movshon, 1997; Morrone, Burr, & Maffei, 1982). V1 neurons are likewise suppressed by stimuli at surrounding locations, i.e., beyond the classical receptive field (Allman, Miezin, & McGuinness, 1985;

Bair, Cavanaugh, & Movshon, 2003; Blakemore & Tobin, 1972; Cavanaugh, Bair, & Movshon, 2002a, 2002b; DeAngelis, Freeman, & Ohzawa, 1994; Levitt & Lund, 1997; Nelson & Frost, 1985). Such suppressive effects have also been found to be dichoptic, e.g., with the preferred and orthogonal gratings presented to separate eyes (Truchard, Ohzawa, & Freeman, 2000; Walker, Ohzawa, & Freeman, 1998).

The normalization model of visual cortical responses was introduced in the early 1990s to explain a variety of such suppressive phenomena evident in the response properties of V1 neurons (Albrecht & Geisler, 1991; Carandini & Heeger, 1994; Carandini et al., 1997; Heeger, 1991, 1992a, 1992b, 1993; Nestares & Heeger, 1997; Tolhurst & Heeger, 1997a, 1997b). The basic idea of the model is that each neuron's response is suppressed by a population of neurons. The suppression is pooled over a larger region of spatial locations and features (e.g., orientations) than the excitatory input. The suppression is divisive such that the excitatory drive from a preferred stimulus is normalized with respect to (divided by) the activity in other neurons that respond to the surrounding context.

Normalization has been proposed as a "canonical" cortical computation (Grossberg, 1973; Heeger, Simoncelli, & Movshon, 1996; Kouh & Poggio, 2008). Analogous suppressive phenomena have been observed in dorsal stream visual cortical areas MT and MST (Britten & Heuer, 1999; Recanzone, Wurtz, & Schwarz, 1997; Snowden, Treue, Erickson, & Andersen, 1991; Treue, Hol & Rauber, 2000), which have been simulated using a model with multiple stages (corresponding to V1 and MT) of summation and normalization (Heeger et al., 1996; Simoncelli & Heeger, 1998). Similar effects have also been described in ventral stream areas V4 and IT (Miller, Gochin, & Gross, 1993; Missal, Vogels, & Orban, 1997; Reynolds, Chelazzi, & Desimone, 1999; Richmond, Wurtz, & Sato, 1983; Rolls & Tovee, 1995; Sato, 1989; Zoccolan, Cox, & DiCarlo, 2005). Normalization of visual cortical responses is analogous to earlier models of retinal light adaptation (Sperling & Sondhi, 1968) and to models of contrast gain control in the retina and LGN (Baccus & Meister, 2002; Bonin, Mante, & Carandini, 2005; Kaplan, Purpura, & Shapley, 1987; Mante, Frazor, Bonin, Geisler, & Carandini, 2005; Shapley & Victor, 1978, 1981). Furthermore, contrast normalization models have been successfully used to characterize results from psychophysical (Boynton & Foley, 1999; Foley, 1994; Foley & Chen, 1997; Meese & Holmes, 2002), visual-evoked potential (Burr & Morrone, 1987; Candy, Skoczenski, & Norcia, 2001; Zhang et al., 2008), and fMRI studies (Boynton, Demb, Glover, & Heeger, 1999) of contrast and spatial vision.

We examined a particular case of cortical normalization in which the visual system is largely invariant to a factor of two change in the excitatory input from LGN, produced by simultaneous stimulation of the two eyes. We measured and compared blood oxygen level dependent (BOLD) fMRI responses evoked by stimulating one or both eyes. We found that V1 responses to binocular stimulation can be explained by a normalization model that assumes mutual suppression between the eyes. Suppression between orthogonal orientations did not depend on the eye of origin, nor on the stimulus onset times, and cross-orientation suppression was weaker than (same orientation) inter-ocular suppression.

Methods

Six volunteers (5 males, 1 female, aged 28–34) participated in the experiments. Observers had normal or corrected-to-normal visual acuity in both eyes and normal stereopsis. Experiments were conducted with the approval of the University Committee on Activities Involving Human Subjects at New York University and following the safety policies and procedures of the NYU Center for Brain Imaging.

Stimuli and visual apparatus

Visual stimuli comprised rings of spiral grating (2 cpd sinusoidal) spanning 1.5 to 2.8 deg eccentricity. The appearance of second order edges was minimized by linearly ramping the contrast from zero to maximum in the inner and outer edges (20 arcmin) of the ring. Stimuli were presented using VisionEgg software (www.visionegg.org). Images were projected onto a rear-projection screen in the bore of the MRI scanner (EIKI LG-XG110, Rancho Santa Margarita, CA). Observers viewed the screen through a mirror haploscope mounted inside the head coil. A septum was installed between the haploscope and the screen to ensure each eye received input only from its corresponding half of the screen.

At the beginning of each session, observers adjusted the haploscope and the position and orientation of the displayed images for each eye to achieve the maximum binocular field of view at their individual neutral vergence. The binocular field of view was slightly larger than 6.5 × 6.5 deg. Observers were instructed to fixate a small square at the center of the binocular field during the whole experiment. A cross hair pattern was presented binocularly around the fixation and a background pattern of static random dots was presented binocularly near the edge of the field of view (6.1 × 6.1 deg) throughout the experiment to facilitate fusion (Figure 1A).

Experimental procedures
Fixation task

Observers were instructed to maintain fixation and attend to a stream of digits appearing at fixation throughout
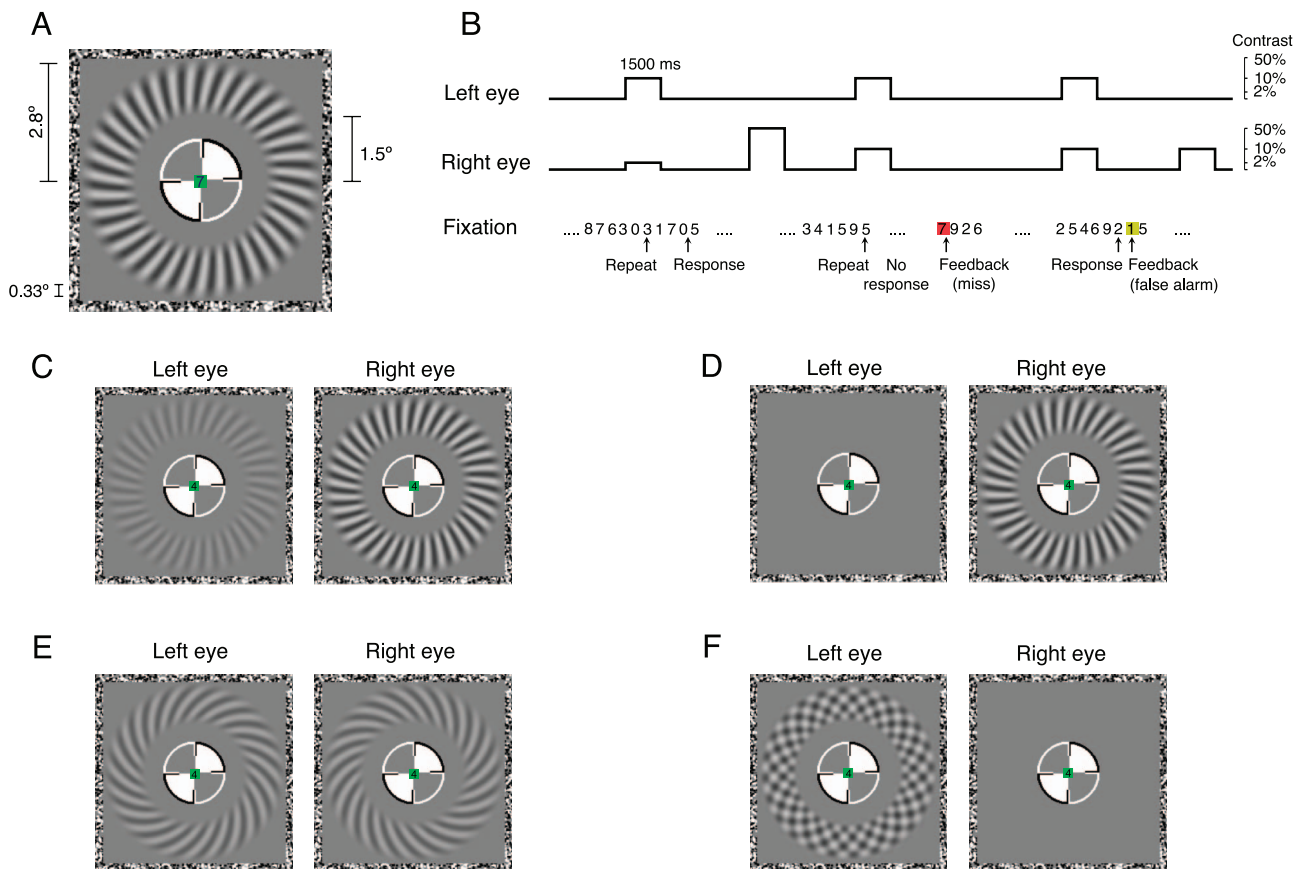
Figure 1. Experimental design. (A) Grating stimuli were presented in the periphery on a gray background while the observer was performing a task on the digits appearing at fixation. Static random dots near the edges of the field of view and a central pattern were continuously present to facilitate binocular fusion. (B) An example of the sequence of events in a run. Five trials are depicted (top two traces); 2nd and 5th trials are monocular trials and the rest are binocular. Trials were presented independently of the central task (bottom row) and were interleaved with blank intervals. Feedback on errors in the central task was given by briefly changing the color of the fixation point to indicate misses (red) and false alarms (yellow). (C) Example of binocular grating (left eye contrast = 2%, right eye contrast = 50%). (D) Example of monocular grating (left eye contrast = 0, right eye contrast = 50%). (E) Example of dichoptic plaid. The two spiral gratings were nearly orthogonal at each point. (F) Example of monocular plaid. The dichoptic and monocular plaids (E and F) were composed of the same spiral grating components.

each run. A random sequence of digits was displayed at a rate of 2 Hz and the observer's task was to continuously monitor them for repetition and to press a key whenever the present digit was identical to the one before the previous one (2-back memory task). Visual feedback was given by briefly changing the color of the fixation point to red if they missed a repetition (no response within 1.5 s after the onset of repeated digit) and to yellow for false alarms. The interval between repetitions was drawn from a uniform random distribution (6–12 s), independent of the timing of the grating stimulus presentations.

Stimulus conditions

There were four stimulus configurations in the series of experiments (Figures 1C–1F, Table 1).

1. Monocular gratings: only one grating was displayed to one eye.
2. Binocular gratings: one grating was shown to each eye; the two gratings had identical spatial frequency, orientation, and phase but could have different contrasts.
3. Dichoptic plaids: one grating was shown to each eye; the two gratings had identical spatial frequency, but locally they were orthogonal to each other.
4. Monocular plaids: two superimposed gratings were presented to one of the two eyes with the other eye blank; the gratings had identical spatial frequency, but they were locally orthogonal.

In the latter three conditions, in all except Experiment 6 (see below), both gratings were displayed simultaneously and for the same duration. Grating stimuli were presented for 1.5 s except in Experiment 3 in which we systematically varied the duration from 0.6 s to 2.4 s.

Trials were interleaved with inter-trial intervals (fixation, background pattern, and central task were present

Experiment	Conditions	Variable	Contrast	N
1	MG	Contrast	1.5–48%	3
2a, 2b	MG vs. BG	Contrast of right eye	Right: 0–50%, Left: 2%, 10%	5, 6
3	MG vs. BG	Duration	50%	4
4	MG vs. DP	Contrast of right eye	Right: 0–50%, Left: 10%	5
5	MG, BG, MP, DP	N/A	10%	6
6	MG, MP, DG (flash suppression)	N/A	10%	5

Table 1. Summary of experiments. *Note*: MG: monocular grating. BG: binocular gratings (compatible). MP: monocular plaid. DP: dichoptic plaid (gratings locally orthogonal). N/A: not applicable to the experiment. *N*: number of observers.

all the time). Trial onsets were distributed randomly (4–8.8 s apart in multiples of 800 ms) and independently from the order of the different stimulus conditions. Each run was balanced in terms of the number of trials for each stimulus condition, but the order of the trials was completely randomized. Trials started 10 s after the beginning of each run. fMRI data were acquired for at least 20 s after the last trial (~6.5 min run for 64 trials).

MRI acquisition

Data were acquired with a Siemens (Erlangen, Germany) 3 Tesla Allegra scanner equipped with a birdcage head coil and a four-channel phased-array surface coil positioned to cover the back of the observer's head (NM-011 transmit and NMSC-021 receive, NOVA Medical, Wakefield, MA).

Functional MRI data were acquired using a T2*-sensitive echo planar imaging (EPI) pulse sequence (repetition time TR = 800 ms, echo time TE = 30 ms, flip angle = 60 deg, 14 slices, voxel size = 3 × 3 × 3 mm).

At the beginning of each scanning session, T1-weighted images were acquired using the same slice prescription as the functional MRI volume using an MPRAGE sequence (slice selective inversion recovery, TR = 1400 ms, TI = 900 ms, TE = 3.79 ms, 18 slices, voxel size = 1.5 × 1.5 × 2.5 mm, 3-mm distance between centers of slices). This T1-weighted volume was used to co-register the fMRI data with a high-resolution structural volume of each observer's brain (Nestares & Heeger, 2000).

The high-resolution T1-weigted images were acquired for each observer in a separate session. Three whole-head MPRAGE (TR = 1.5 s, TI = 900 ms, TE = 3 ms, flip angle = 10 deg, voxel size = 1 × 1 × 1 mm) scans were acquired using the birdcage coil, co-registered and averaged, and the resulting structural images were used for gray/white matter segmentation and cortical flattening.

Defining regions of interest in visual cortex

Retinotopic mapping data were acquired, for each observer, in a separate session. Borders between visual areas were identified based on reversals of the polar angle maps (DeYoe et al., 1996; Engel, Glover, & Wandell, 1997; Engel et al., 1994; Sereno et al., 1995).

In addition, a localizer experiment was used to identify the subregions of each visual area corresponding to the stimulus annulus. Each scanning session began with a localizer run in which a flickering (10 Hz) square-wave grating (2 cpd) was displayed to the left eye and the right eye in alternating epochs. Each eye was stimulated for 10 s followed by 10-s fixation and background pattern. Five such epochs were collected for each eye after an initial delay of 6 s. Activation of voxels in the localizer run was used in conjunction with the borders from retinotopic mapping to define three regions of interest (V1, V2, and V3, Table 2). In a subset of sessions, we collected two localizer runs and averaged them to improve the selection of ROIs.

Data analysis
Preprocessing

The fMRI time series were motion corrected within and between scans assuming a rigid-body transformation (Jenkinson, Bannister, Brady, & Smith, 2002). The time series of each voxel was high-pass filtered (cut off = 0.01 Hz) to remove drift and normalized by its mean intensity to compensate for variations in intensity with distance from the surface coil and to convert the data from arbitrary image intensity units to percentage signal change.

Localizer

The localizer data were analyzed by fitting the time course of each voxel with two sinusoids, with periods of

Area	Mean ROI size (mm^3)	SD across observers and sessions (mm^3)
V1	2551	1160
V2	3493	1560
V3	3304	1437

Table 2. Sizes of regions of interest, averaged across observers and sessions.

Experiment	Mean	Range
1	44	32–48
2a	64	56–72
2b	60	48–64
3	62	56–72
4	62.4	56–64
5	125.3	112–128
6	172	120–216

Table 3. Number of trials per condition.

20 s (for eye-independent activation) and 40 s (for eye-dependent activation). ROIs were restricted to include voxels with responses that correlated with the eye-independent (20-s period) sinusoid. Voxels were included in the ROI if the correlation exceeded $r > 0.35$ for one localizer run or $r > 0.5$ if two localizer runs were collected and averaged, and if the response phase was between 0 and pi. We did not find any significant and reliable ocular bias, i.e., there was no significant correlation with the eye-dependent sinusoid (40-s period). Hence, there was no evidence that any voxels responded more or less strongly to one eye or the other and attempts to "read out" eye of origin using a classifier analysis (Haynes & Rees, 2005a, 2005b; Kamitani & Tong, 2005) yielded chance performance.

Response time courses, response amplitudes, and total activity

The mean fMRI response time course, evoked by each stimulus condition in the main experiments, was estimated using deconvolution (Buracas & Boynton, 2002; Dale, 1999). To estimate hemodynamic responses with maximum lengths of $t \times TR$ from n measurements for each voxel, an $n \times t$ design matrix M was constructed for each condition as follows: $M_{i,j} = 1$ if a trial of the corresponding condition started during the $(i - j + 1)$th measurement, and $M_{i,j} = 0$, otherwise. We then applied a high-pass filter (described above) to the columns of the design matrix and used the resulting matrices as regressors. The resulting (deconvolved) fMRI response time courses were corrected for baseline shifts by subtracting the mean of the first 3 time points (corresponding to the initial 2.4 s after stimulus onset) and were plotted and compared across conditions. For Experiment 3, "total activity" was computed as the integral, from 2.4 s after stimulus onset to 12 s after stimulus offset, of the deconvolved response time courses (comprising mostly the positive part of the response). Number of trials for each condition is shown in Table 3.

In a complementary analysis of the data, response amplitudes were estimated using a general linear model (GLM), assuming a hemodynamic impulse response function (HRF) expressed as a difference of two gamma functions. For each condition, a regressor was constructed by convolving the HRF with a boxcar function describing the presence or absence of the stimulus as a function of time. The resulting function was downsampled to the sampling rate of measurements (TR = 800 ms) and then a high-pass filter was applied to the resulting regressor (as was done in preprocessing the data). For each observer, parameters determining the shape of the HRF were fitted to the mean response time course (computed with deconvolution), averaged across sessions, stimulus conditions, and ROIs. Response amplitudes and total activity were calculated for each stimulus condition by multiplying the estimated coefficient with the original regressor (corresponding to one trial of that condition, prior to high-pass filtering) and taking the peak, or the area under the response curve, respectively.

Response time courses (from deconvolution), response amplitudes (from GLM), and total activity estimates (from both analyses) were averaged across voxels within each ROI and across observers. Variability across observers was quantified as the standard error of the mean. Only for the analysis pertaining to Figures 2 and 4 (Experiments 1 and 2), we scaled the responses from each observer, before averaging across observers, to minimize the inter-subject differences in the monocular responses. A scale factor for each observer was estimated using linear regression; specifically, the monocular responses were regressed against a sigmoid curve. Responses were then divided by this factor, so that the minimum and maximum monocular responses spanned zero to one for all observers. The same scale factors were then used for the binocular responses. Note that this scaling did not change the shape parameters of the contrast response functions (p and σ in Equation 2) and it did not depend on the responses to binocular stimulus conditions.
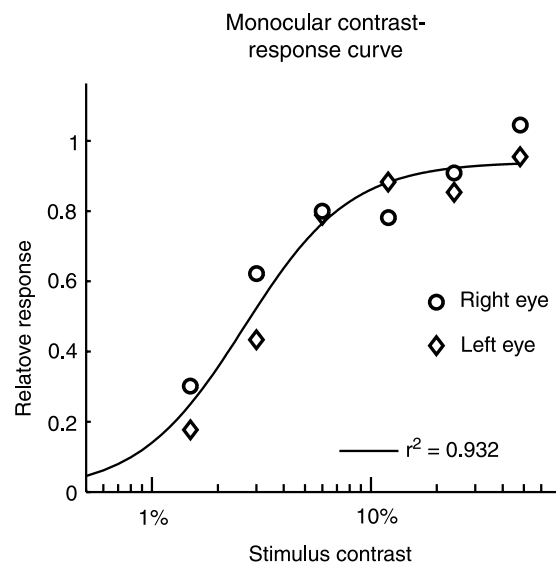

Figure 2. V1 monocular contrast response curve, averaged across three observers (Experiment 1). Solid curve, model fit based on Equation 2.

Statistical significance was determined by performing multi-way analysis of variance (observer × condition or observer × visual area × condition with observer as random effect) followed by Fisher's least significant difference (LSD) test between conditions of interest.

Additivity index

An additivity index was defined to quantify the failure of additivity of the responses to pairs of gratings. Specifically, we computed

$$AI(c) = \frac{r(c_{ref}, c) - r(0, c)}{0.5 \times [r(c_{ref}, 0) + r(0, c_{ref})]}, \quad (1)$$

where $r(c_L, c_R)$ was the response evoked by left eye contrast c_L and right eye contrast c_R, and c_{ref} denotes the reference contrast (e.g., 2% or 10% in Experiments 2a and 2b, respectively). We assumed that the monocular responses were equal for both eyes, that is, $r(0, c) = r(c, 0)$. Averaging the monocular responses, therefore, minimized estimation error in the denominator. A value of 1 for the index implied additivity, such that the response to the sum of two gratings equaled the sum of the two responses to each grating individually.

Models

Monocular contrast normalization

The contrast normalization model posits that, for a single monocular grating stimulus, the response r as a function of grating contrast c is given by

$$r(c) = a \frac{c^n}{c^n + \sigma^n}, \quad (2)$$

where a determines the amplitude, and n and σ determine the shape of the sigmoid contrast response curve. Equations of this form have been fitted previously to data from single-unit electrophysiology, psychophysics, fMRI, and visual-evoked potential experiments (see Introduction section for references). We used Equation 2 to fit the responses evoked by monocular gratings.

The data from the binocular stimulus conditions were then used to distinguish between several alternative models of binocular interactions. Each of these models assumes that the fMRI responses reflect the pooled activity of a population of neurons, driven by inputs to one or the other or both eyes, and all different grating orientations. Adding a second grating will typically evoke more activity in one subpopulation of neurons even though it may strongly suppress activity in another subpopulation. Hence, the models predict that the fMRI response to a pair of gratings (whether presented to the same or different eyes, with the same or different

orientations) will be greater than or equal to the response to a single monocular grating component.

Linear binocular summation

If inputs from the left and right eyes do not interact, then the responses evoked for left eye contrast c_L and right eye contrast c_R are

$$r(c_L, c_R) = a \frac{c_L^n}{c_L^n + \sigma^n} + a \frac{c_R^n}{c_R^n + \sigma^n}, \quad (3)$$

or alternatively,

$$r(c_L, c_R) = r(c_L) + r(c_R), \quad (4)$$

i.e., the binocular responses are the sum of the monocular responses. This linear summation model assumes that any hemodynamic nonlinearity is negligible, and that the responses to left and right eye stimulations are about equal. This model predicts that the additivity index would always be equal to one.

Nonlinear binocular summation

There are several possible scenarios for how left and right eye inputs might interact nonlinearly. According to the nonlinear summation model, the fMRI response amplitudes are

$$r(c_L, c_R) = a \frac{f(c_L, c_R)^n}{f(c_L, c_R)^n + \sigma^n}, \quad (5)$$

where f describes how inputs from the left and right eyes are combined prior to normalization. To maintain the fit for monocular inputs f needs to satisfy the constraint $f(c, 0) = f(0, c) = c$. That is, if the contrast in one eye is zero, then Equation 5 reduces to Equation 2. Reasonable choices for such a function are linear summation, i.e., $f(c_L, c_R) = c_L + c_R$, or subadditive functions such as $f(c_L, c_R) = (c_L^2 + c_R^2)^{1/2}$ or $f(c_L, c_R) = \max(c_L, c_R)$. Note, however, that even if f is linear, the overall interaction is nonlinear. Equation 5 assumes that all cortical neurons are binocular, with no contribution from monocular neurons to the pooled activity as measured with fMRI.

Binocular normalization

Alternatively, the binocular normalization model assumes that inputs from each eye contribute equally to the normalization for both eyes, i.e.,

$$\begin{aligned} r(c_L, c_R) &= a \frac{c_L^n}{c_L^n + c_R^n + \sigma^n} + a \frac{c_R^n}{c_L^n + c_R^n + \sigma^n} \\ &= a \frac{c_L^n + c_R^n}{c_L^n + c_R^n + \sigma^n}. \end{aligned} \quad (6)$$

This model allows for contributions from monocular neurons (driven by one eye but suppressed by both, as in one or the other term in the top line of the equation) and/or binocular neurons (driven by both eyes and suppressed by both, as in the bottom line of the equation).

Power law

Finally, power-law nonlinearity after linear binocular summation results in a sublinear summation of fMRI responses. According to this model, the fMRI response amplitude is a power-law function of the underlying *neural* activity. Thus, monocular response amplitudes are

$$r(c) = R(c)^k, \tag{7}$$

where $r(c)$ is the fMRI response to a monocular grating, $R(c)$ is the underlying neural activity, pooled across the population of neurons corresponding to that eye, and k is the power-law exponent. Binocular response amplitudes are

$$r(c_L, c_R) = [R(c_L) + R(c_R)]^k. \tag{8}$$

One can describe the relationship between monocular and binocular response amplitudes directly as

$$r(c_L, c_R) = [r(c_L)^{1/k} + r(c_R)^{1/k}]^k. \tag{9}$$

This model was used to assess the possibility that the total activity in the underlying neural responses increased linearly with stimulus duration but that the hemodynamics exhibited a saturating nonlinearity (see Experiment 3: Contribution from hemodynamic nonlinearity section).

Results

Inter-ocular suppression from compatible stimuli

Experiment 1: Monocular contrast response function

We focus initially on the fMRI responses in V1 (a similar pattern was seen in V2 and V3, see Inter-ocular suppression in extrastriate visual areas section). To have a baseline of comparison for the responses to binocular gratings (Experiments 2a and 2b, below), we measured cortical activity as a function of contrast to single monocular gratings. Monocular responses were measured for six contrast levels (1.5, 3, 6, 12, 24, and 48%) presented separately to the right and left eyes (Figure 2). We scaled the response amplitudes from each observer, before averaging across observers, to minimize the inter-subject differences in the monocular responses (see Data analysis section); these same scale factors were then used for the binocular responses presented below (Figure 4).

The monocular contrast normalization model (Equation 2) was used to fit the monocular responses, with three free parameters (a, n, and σ), by performing a numerical search to minimize squared error. The fit accounted for the responses well ($R^2 = 0.93$, Figure 2). The best-fit values of parameters were: $a = 0.98$ (because the data were rescaled to approximately span zero to one before fitting), $\sigma = 3.6\%$ contrast, and $n = 1.7$. These parameters were hereafter fixed for the analysis of the data from subsequent experiments.

Experiment 2: Failure of additivity

The contrast of the grating presented to the right eye was varied (0, 2, 10, or 50%) while keeping the contrast of the grating presented to the left eye constant (0% in the monocular condition, and 2% or 10% in the binocular conditions).

The fMRI response to a pair of gratings (whether presented to the same or different eyes, with the same or different orientations) will generally be greater than or equal to the response to a single monocular grating component. fMRI responses reflect the pooled activity of cortical neurons, which are driven by inputs to one or the other or both eyes, and all different grating orientations. Adding a second grating will evoke more activity in one subpopulation of neurons even though it may strongly suppress activity in another subpopulation of neurons. The signature of suppression, therefore, was a failure of additivity rather than a net decrease in the fMRI responses.

The responses were not additive; the response to the sum of two gratings was generally less than the sum of the responses to each grating presented individually. For both monocular stimulation (0% left eye contrast) and binocular stimulation (2% or 10% left eye contrasts in Experiments 2a and 2b, respectively), fMRI responses increased with the contrast of the right eye grating (Figure 3A). In the binocular conditions, however, the responses for different right eye contrasts spanned a much smaller range than in the monocular condition. The maximum binocular response was not noticeably higher than the maximum monocular response (Figure 3A, 50% right eye contrast, compare black curves in the left and right panels).

An additivity index was defined as the relative difference between binocular and monocular activities, to quantify the failure of additivity (see Additivity index section). A value of 1 for the index implied additivity, such that the response to the sum of two gratings equaled the sum of the two responses to each grating individually. For both left eye contrasts (2% and 10%), the responses were subadditive (additivity index <1); superimposing the left eye grating had a smaller effect on the responses when the right eye contrast was higher (Figure 3B). Indeed, the additivity index was inversely related to the right eye contrast, i.e., inversely related to the activity evoked by right eye stimulation on its own.
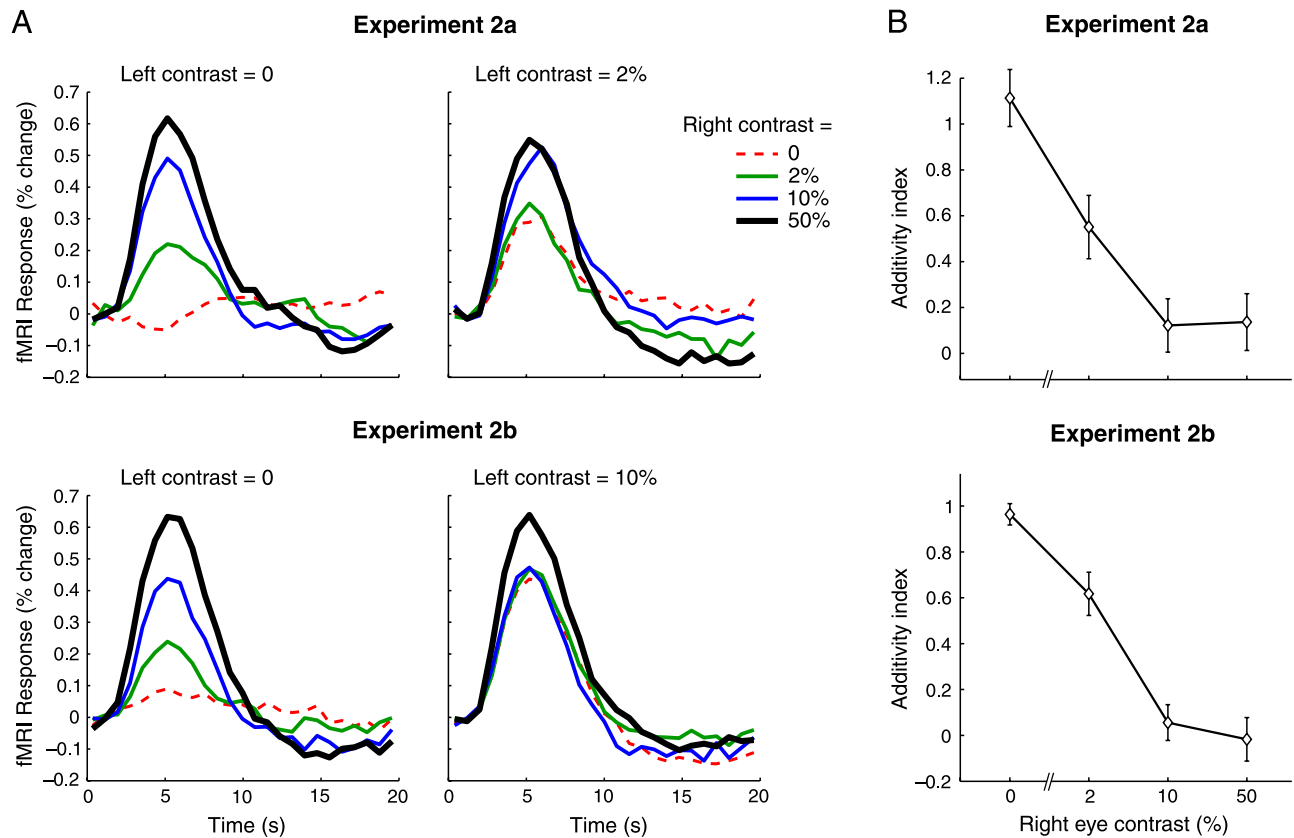
Figure 3. Failure of additivity. (A) Average V1 response time courses to monocular (left) and binocular (right) gratings in Experiments 2a (top panels) and 2b (bottom panels). The ordinate represents percent change in the intensity of the fMRI measurements averaged across all voxels in the V1 region of interest, and averaged across observers. (B) Additivity index as a function of right eye contrast. The ordinate represents the relative difference between binocular (left eye stimulus present) vs. monocular (left eye stimulus absent) responses (Equation 1). Error bars represent standard error of mean (*SEM*) across observers.

Model comparisons

The data were used to distinguish between several alternative models of binocular interactions (see Models section). The linear binocular summation model, the nonlinear binocular summation model, and the binocular normalization model (Equations 3–6) were without free parameters; the parameters were estimated from the monocular responses in Experiment 1 and were assumed to be observer-independent. For the power-law model (Equation 9), one additional parameter (k, the exponent of the power-law) was estimated independently from Experiment 3 (see below).

The linear binocular summation model (Equation 3) predicted that the additivity index would always be equal to one, which failed to explain why the response to a stimulus in one eye depended on the contrast of the stimulus in the other eye.

Binocular normalization (Equation 6) provided a better fit to the data than did linear binocular summation (Equation 3), as shown in Figure 4. The binocular normalization model fit the data well (Figure 4, left

panel). The linear binocular summation model did poorly in accounting for the results of Experiment 2b (Figure 4, middle panel).

Binocular normalization also provided a better fit than did the power-law model (Equation 9). The power-law model was like the linear binocular summation model but allowed for a power-law hemodynamic nonlinearity. Even with the power-law nonlinearity (with k estimated from Experiment 3), the predicted binocular responses were still much larger than the observed responses (Figure 4, right panel).

Good fits to the data were also obtained using the nonlinear binocular summation model (Equation 5). The best-fit curves using Equation 5 (using three different functions f: sum, root sum square, and maximum of input contrasts) were very similar to those obtained using the binocular normalization model (Equation 6). Hence, our data are compatible with the existence of suppressive inter-ocular interactions in V1 but do not clearly distinguish between these different functional forms for the interactions.
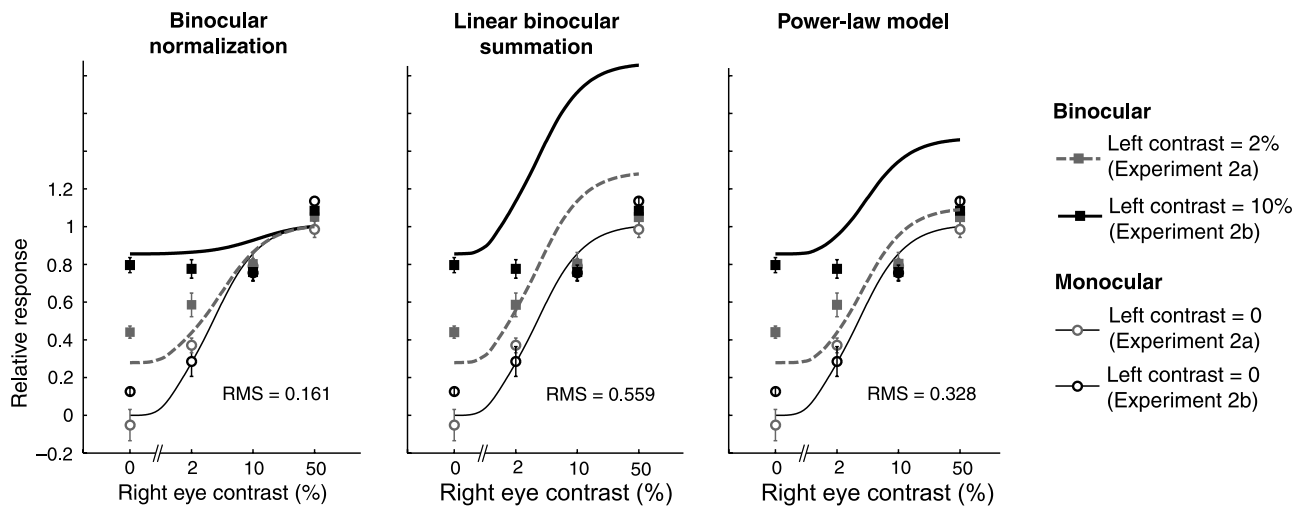
Figure 4. Binocular contrast normalization vs. linear summation of monocular responses. Predictions from three models of inter-ocular interactions are plotted along with the V1 measurements (averaged across five observers) from Experiments 2a (left eye contrast 2%) and 2b (left eye contrast 10%). Open symbols: monocular responses. Solid symbols: binocular responses. The thin curve is the same as the monocular response curve in Figure 2. Thick curves depict predictions of different models. *Left panel*: The binocular normalization model (Equation 6). *Middle panel*: Linear binocular summation model consisting of monocular normalization followed by linear binocular summation (Equation 3). *Right panel*: Power-law model consisting of monocular normalization with linear binocular summation and power-law hemodynamic nonlinearity (Equation 9). Error bars represent *SEM* across observers. Root mean square (RMS) error for binocular conditions (i.e., the upper two curves in each panel) is reported for each model.

Experiment 3: Contribution from hemodynamic nonlinearity

The aims of this experiment were twofold. First, we examined whether or not there was evidence for a nonlinearity in the hemodynamics underlying the fMRI responses (or equivalently, linear summation of the inputs from the two eyes followed by saturation of the underlying neural responses). Second, additivity of the responses was assessed for different response levels but at a fixed contrast. Experiment 3 was similar to Experiment 2 except that the gratings were presented for various

durations (0.6, 1.2, 1.8, or 2.4 s), and the contrast presented to each eye was fixed at 50%. In the binocular condition, the two gratings were identical.

Increasing the duration of the stimulus resulted in larger and longer fMRI responses (Figure 5). The peak amplitudes of the response time courses and the durations of the responses increased monotonically with stimulus duration (Figure 5A). The peak amplitudes did not differ by much for the longest two durations (1.8 s vs. 2.4 s), but this was qualitatively consistent with what one would expect of a linear system (low-pass filter or leaky integrator); consider
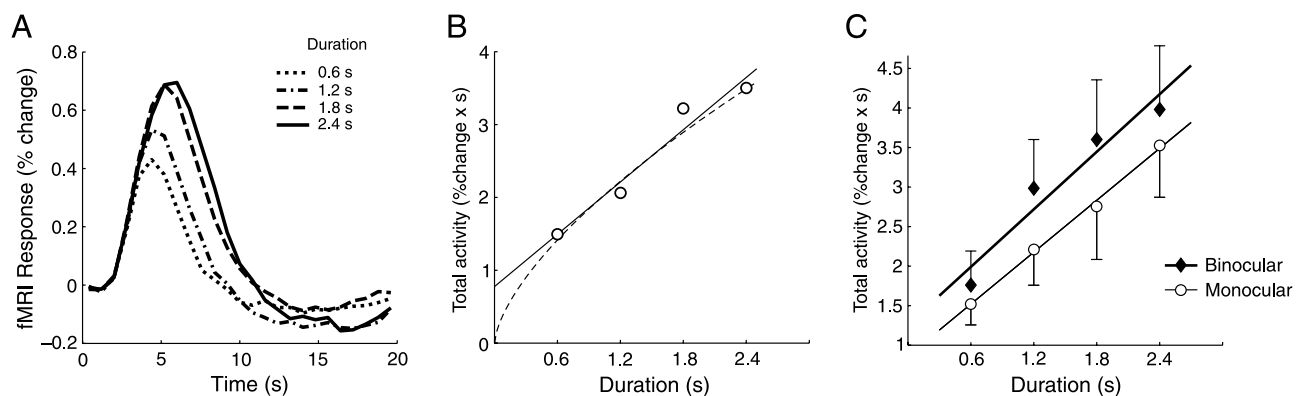

Figure 5. V1 responses increased with the duration of stimulus presentation. (A) Average V1 response time courses, averaged across 4 observers, for 4 stimulus durations. Responses for monocular and binocular trials were similar and were, therefore, averaged together. (B) Total activity quantified as the integral, from 2.4 s after stimulus onset to 12 s after stimulus offset, of the mean response time courses in panel A. Solid line and dashed curve depict the best-fit line and power law, respectively. (C) Total activity using a complementary GLM analysis for both monocular (filled symbols) and binocular (open symbols) stimulation. Error bars indicate *SEM* across observers.

by analogy the step response of an RC circuit as a function of the step duration. Importantly, response durations continued to increase with stimulus duration, even when the peak amplitude no longer did so.

Hence, the peak response amplitude was not an appropriate measure for assessing nonlinearities in the responses (nor would it be for an RC circuit). The linearity of the responses was, therefore, quantified using two complementary analyses (see Data analysis section) that assessed the total amount of activity (which depends on both peak and duration) for each duration. First, the total activity was computed as the integral of the mean response time courses (Figure 5B). Second, a general linear model assuming a canonical low-pass filter for the hemodynamics was used to estimate the underlying neural response amplitude for each stimulus duration. This underlying response amplitude was then multiplied by the stimulus durations to yield a measure of the total activity (Figure 5C). For both analyses, the total activity was well fit by a line (Figure 5B: $R^2 = 0.91$; Figure 5C, monocular: $R^2 = 0.99$; Figure 5C, binocular: $R^2 = 0.93$).

Both monocular and binocular conditions followed a very similar linear trend (Figure 5C). Although adding the left eye stimulus tended to increase the total activity, the overall difference between monocular and binocular responses was not quite statistically significant (three-way ANOVA, observer $\times$ duration $\times$ binocularity: $F(1,9) = 8.29$, $p = 0.06$), and this effect was not systematically reduced for longer stimulus presentations, i.e., the inter-action between larger responses (due to longer stimulation duration) and binocularity was not significant (interaction between duration and binocularity: $F(3,9) = 1.47$, $p = 0.29$).

The increase in total activity as a function of stimulus duration was very well fit with a line. Nonetheless, the positive intercept of the line suggests a nonlinear response component for short stimulus durations (shorter than 0.6 s). One possible explanation for this behavior is that the underlying neural activity exhibited strong transient responses at stimulus onset followed by rapid adaptation of neural responses (Boynton, Engel, Glover, & Heeger, 1996).

An alternative possibility, however, is that the total activity in the underlying neural responses increased linearly with stimulus duration but that the hemodynamics exhibited a nonlinearity. To assess this possibility, we fit the data from Experiment 3 with a power function of the form x^k, where k was the exponent, and x was proportional to the duration of the stimulus. Nonlinear least squares was used to estimate k that best fit the results in Figure 5B (dashed curve, $k = 0.65$). The nonlinear fit was as good as the line fit ($R^2 = 0.91$ for both fits, where R^2 is the coefficient of determination). Good fits were also obtained to the total activity estimates from GLM analysis (Figure 5C, monocular: $k = 0.63$, $R^2 = 0.99$; Figure 5C, binocular: $k = 0.54$, $R^2 = 0.96$). However, a simultaneous fit of the monocular and binocular responses did not fit as well. Assuming that the response to monocular stimuli is x^k and the response to binocular

stimuli is $(2x)^k$, the best fit to the data was obtained with $k = 0.47$ ($R^2 = 0.91$).

Regardless, the power-law model could not explain the failure of additivity in Experiment 2. The power-law nonlinearity predicts that the additivity index should have been $2^k - 1$ when the contrasts of left eye and right eye were equal, regardless of the contrast, that is, between 0.46 and 0.57 depending on the estimate of k (0.47–0.65, see preceding paragraph). The measured additivity index (averaged across observers) in Experiment 2b for 10% contrast (both left and right eyes) was only 0.01 (95% confidence interval = −0.23 to 0.25). Moreover, a power-law nonlinearity when coupled with linear binocular summation failed to fit the data from Experiment 2 (Figure 4, right panel). Thus, a power-law hemodynamic nonlinearity failed to account for the combined results of Experiments 1–3, and the alternative explanation must be accepted, that the failure of additivity reflected contrast-dependent neural interactions, such as normalization.

Inter-ocular suppression from orthogonal gratings

Experiment 4: Dichoptic plaids vs. binocular gratings

Experiment 4 was performed to determine if the suppression depended on orientation. fMRI responses were measured as a function of the contrast of the grating presented to the right eye (0, 2, 10, or 50%) in two conditions: monocular (0% left eye contrast) and binocular (10% left eye contrast). Unlike Experiment 2, the two gratings were locally orthogonal everywhere, forming a dichoptic plaid. Such plaids drive two subpopulations of orientation-selective neurons.

Figures 6A and 6B compare responses to single vs. two orthogonal gratings, respectively. The monocular condition (Figure 6A) was essentially identical to that in Experiment 2, and the monocular responses were the same as in Experiments 2a and 2b, as expected. Adding the left eye stimulus resulted in larger responses, especially for low (2%) right eye contrast (compare green curves in Figures 6A and 6B), but also for higher (10%, 50%) right eye contrasts (compare blue and black curves, respectively, in Figures 6A and 6B). In Experiment 2 (Figure 3), by comparison, adding the left eye stimulus resulted in larger responses only when the right eye contrast was low (2%). Overall, responses to incompatible stimuli in Experiment 4 were larger (exhibiting less suppression) than those evoked by compatible stimuli in Experiment 2 (Figure 6C), that is, suppression from incompatible, dichoptic plaids was weaker than that observed for compatible gratings. This finding suggests that the mechanisms underlying response normalization for binocular inputs are orientation selective. There was, even so, a clear failure of additivity when orthogonal stimuli were presented to the two eyes. The additivity index of about 0.5 at high contrasts meant that the response increment
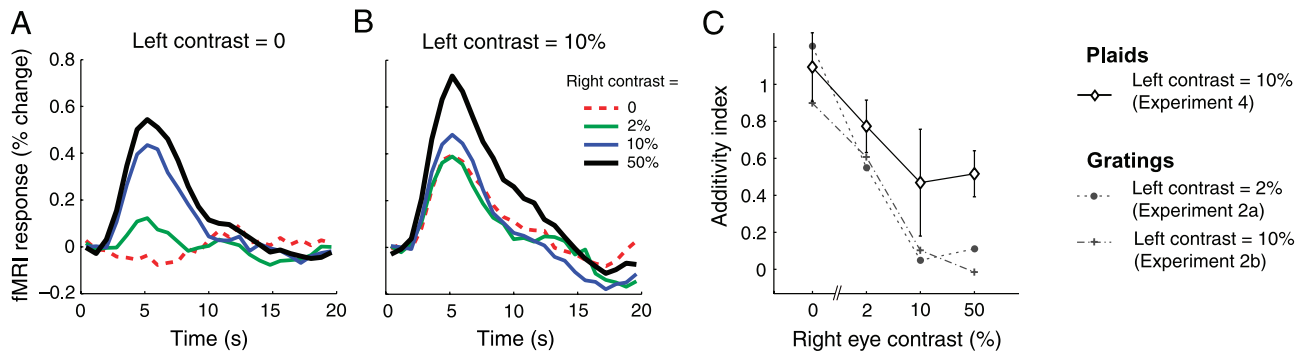
Figure 6. Dichoptic plaids vs. binocular gratings. (A) Average V1 response time courses to monocular gratings. (B) Average V1 response time courses to dichoptic plaids composed of two orthogonal gratings. (C) Additivity index as a function of right eye contrast, both for orthogonal gratings composing a dichoptic plaid (solid curve, open symbols) and for compatible gratings (Experiment 2, dashed curves, filled symbols, copied from Figure 3). Error bars represent *SEM* across observers.

evoked by presenting a left eye stimulus along with the right eye stimulus was only about one half the response evoked by the left eye stimulus on its own. A single static nonlinearity does not explain the difference between collinear and orthogonal gratings. One needs to introduce additional terms to Equation 5 or Equation 6 to account for such a difference. For example, the normalization model can be generalized to explain responses to incompatible stimuli by assuming unequal contributions from the same vs. different orientations in the normalization:

$$r(c_L, c_R) = a \frac{c_L^n}{c_L^n + wc_R^n + \sigma^n} + a \frac{c_R^n}{c_R^n + wc_L^n + \sigma^n}, \qquad (10)$$

where w depends on the orientation difference between the two gratings. For collinear orientations, we assumed $w = 1$ (see Equation 6). For orthogonal orientations, a good fit to the data from Experiment 4 was obtained with $w = 0.52$ ($R^2 = 0.83$).

This failure of additivity can be attributed to inter-ocular suppression, cross-orientation suppression, or a combination of the two. These possibilities were examined in Experiment 5. It should be noted, however, that the additivity index of about 0.5 could also be explained by a power-law hemodynamic nonlinearity (see Experiment 3: Contribution from hemodynamic nonlinearity section).

Experiment 5: Dichoptic vs. monocular plaids

We directly compared binocular and cross-orientation suppression by measuring responses to the following four stimulus conditions:

1. monocular gratings (one grating was presented to either the left or the right eye),
2. binocular gratings (identical gratings were presented to both eyes),
3. monocular plaids (two superimposed orthogonal gratings were presented to one eye), and

4. dichoptic plaids (two orthogonal gratings were presented to the two eyes).

The contrasts of the gratings were fixed at 10%. Results are depicted in Figure 7.

The responses to these four stimulus conditions differed significantly ($F(3,15) = 8.27$, $p = 0.0018$, 2-way ANOVA). Among the four conditions, a single grating (monocular grating) evoked the smallest responses, significantly smaller than the responses to two orthogonal gratings (monocular and dichoptic plaids, $p < 0.05$), and slightly (though not significantly) smaller than the responses to two identical gratings (binocular gratings). Binocular compatible gratings evoked responses that were smaller than those evoked by monocular plaids ($p < 0.05$), and slightly (though not significantly) smaller than the responses to dichoptic plaids. Responses to dichoptic plaids were slightly (though not significantly) smaller than the responses to monocular plaids. The additivity indexes for the responses plotted in Figure 7B were 0.15 for binocular gratings, 0.31 for dichoptic plaids, and 0.47 for monocular plaids.

In sum, when a grating was presented to one eye, adding a compatible grating to the other eye only slightly increased the responses, whereas adding an orthogonal grating, to the same eye or to the other eye, significantly increased (although far short of doubling) the responses.

Experiment 6: Flash suppression of incompatible stimuli

Incompatible images presented to different eyes might be expected to evoke responses that compete and suppress each other particularly strongly. The trend seen in Figure 7 for responses to dichoptic plaids to be smaller than monocular plaids was not statistically significant, however, so we set out to maximize the interaction between the two eyes using a well-known psychophysical technique called flash suppression (Wolfe, 1984). Introducing a short temporal delay between the onsets of incompatible stimuli presented to the two eyes results in a robust and
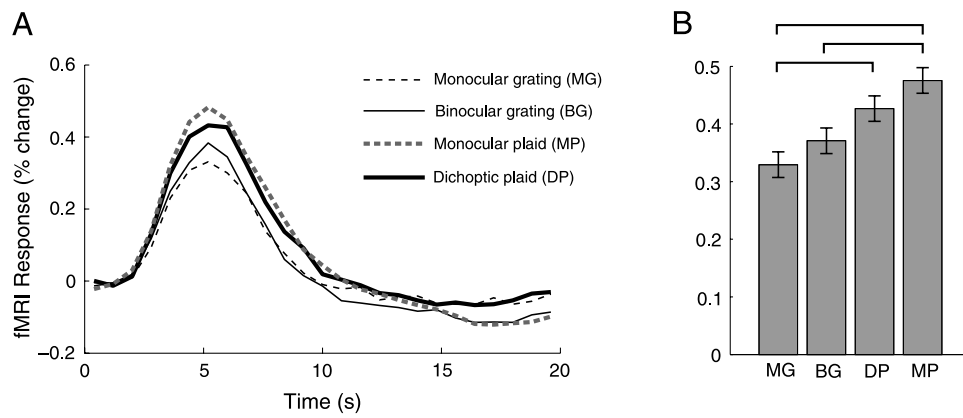
Figure 7. Responses to monocular and binocular gratings and plaids, and dichoptic plaids. (A) Average V1 response time courses to one or two superimposed gratings, presented to one (monocular) or both (binocular or dichoptic) eyes. (B) Response amplitudes for each of the four conditions. Error bars represent *SEM* across observers. Brackets indicate statistically significant differences ($p < 0.05$).
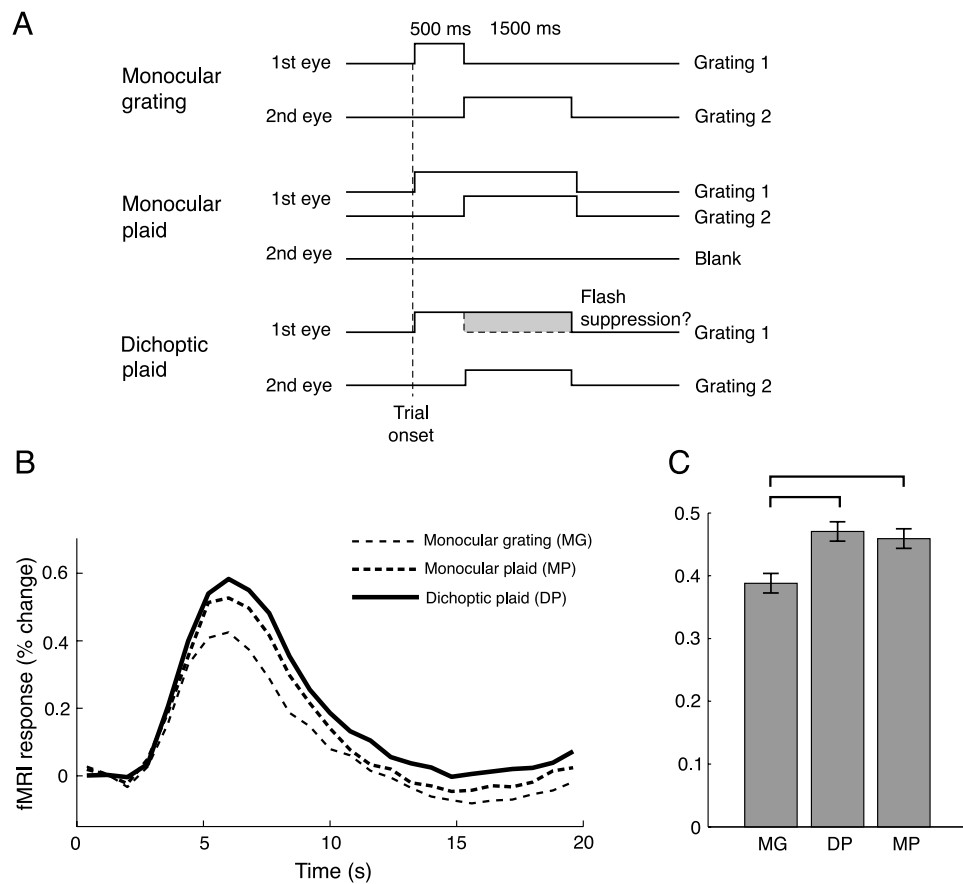

Figure 8. Failure to induce flash suppression of fMRI responses. (A) Time course of stimulus presentations for each of the three conditions. Each trial began by presenting a grating to one eye. A second grating, locally orthogonal to the first one, was displayed after 500 ms. In monocular grating (MG) trials, the first grating was removed and the second grating was presented to the other eye. In monocular plaid (MP) trials, the first grating remained and the second grating was superimposed with it. In dichoptic plaid (DP) trials, the first grating remained while the second grating was displayed to the other eye. In this case, if attention had not been diverted by the central fixation task, observers would have experienced perceptual suppression of the first grating. (B) Average V1 response time courses evoked by these conditions. (C) Comparing the response amplitudes failed to reveal greater suppression for dichoptic plaids. Error bars represent *SEM* across observers. Brackets indicate statistically significant differences ($p < 0.05$).

controlled form of perceptual suppression, in which the first stimulus disappears and the second stimulus dominates the percept.

Three different conditions were compared (Figure 8A). In monocular grating trials, a grating was presented to one eye for 500 ms, and then a second grating was presented to the other eye for 1500 ms. Presentation of the two gratings did not overlap temporally and therefore there was no interaction or competition between responses to the gratings. In monocular and dichoptic plaid trials, the first grating was presented for 2 s, the last 1.5 s of which temporally overlapped with a second, orthogonal grating. In monocular plaid trials, the two gratings were presented to the same eye; therefore, there was no inter-ocular interaction between them although there could have been cross-orientation suppression. In dichoptic plaid trials, orthogonal gratings were presented to different eyes, possibly eliciting inter-ocular interactions, which might have resulted in stronger suppression of V1 responses. As in all of the preceding experiments, observers performed a demanding task at fixation, thereby diverting their attention from the grating and plaid stimuli. In terms of the physical stimulus contrasts, dichoptic plaid trials were

similar to the monocular plaid trials. However, had observers been viewing the gratings (instead of doing the central fixation task), their perceptual experience in dichoptic plaid trials would have been similar to monocular grating trials because of flash suppression.

Consistent with Experiment 5, the responses were significantly different across conditions ($F(2,8) = 8.29$, $p = 0.0112$, 2-way ANOVA). Specifically, the responses to plaids (both dichoptic and monocular) were larger than the responses to monocular gratings. There was, however, no evidence of stronger suppression for dichoptic than monocular plaids. The responses to monocular and dichoptic plaids were almost equal, and the trend seen in Experiment 5 (greater responses to monocular than dichoptic plaids) was not replicated. We thus failed to find evidence for a neural correlate of flash suppression in the measured V1 activity.

Inter-ocular suppression in extrastriate visual areas

The profile of responses in V2 and V3 was in general similar to that in V1, for all of the experiments. Figure 9A
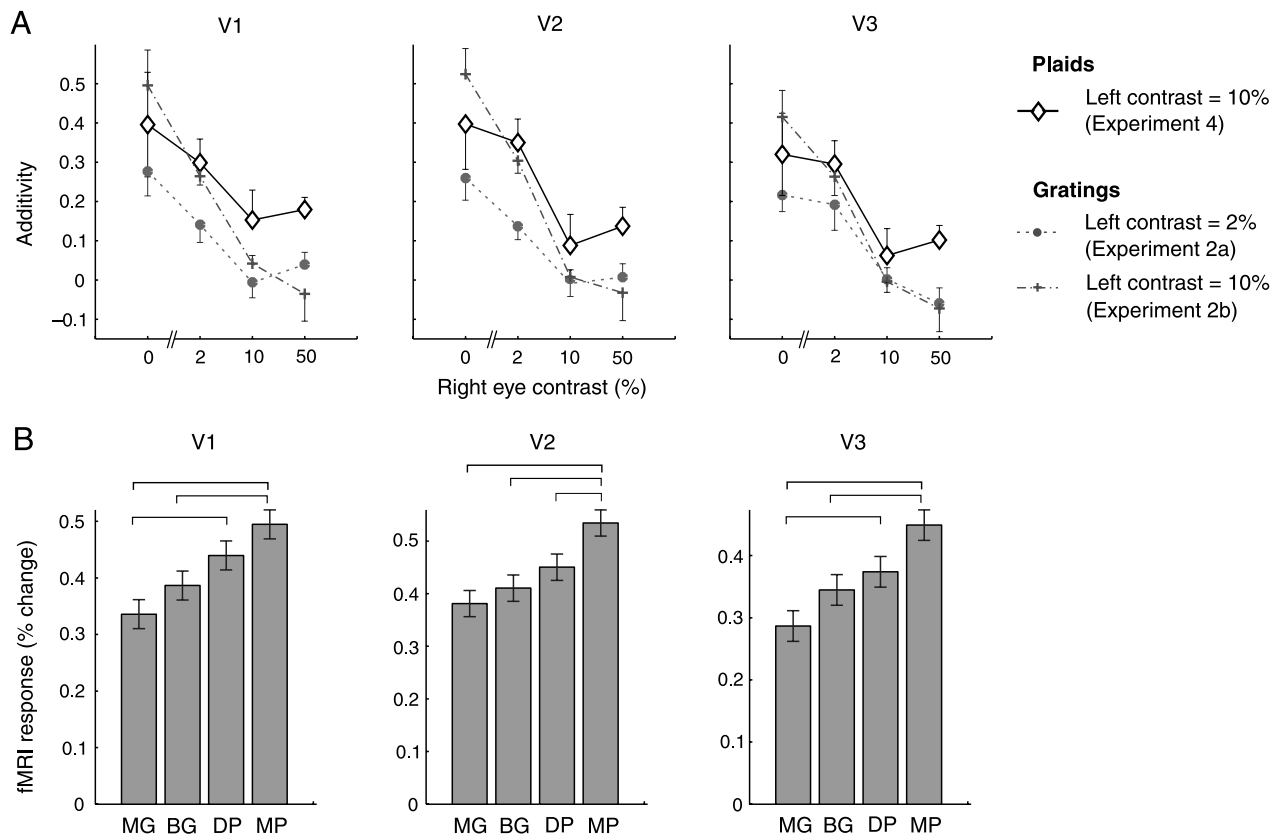

Figure 9. Similar pattern of responses observed in V1, V2, and V3. (A) Additivity (the numerator in Equation 1) for binocular gratings (Experiment 2) and dichoptic plaids (Experiment 4), as a function of right eye contrast. V1 responses replotted from Figures 3 and 6. Error bars, *SEM*. (B) Responses to monocular and binocular gratings and plaids, and dichoptic plaids (Experiment 5). V1 responses replotted from Figure 7. Monocular and binocular gratings evoked smaller responses than monocular plaids in all three visual areas. Responses evoked by dichoptic plaids were statistically indistinguishable from those evoked by binocular gratings and monocular plaids. Error bars represent *SEM* across observers. Brackets indicate statistically significant differences ($p < 0.05$).

compares the activity of V1–V3 for Experiment 2 (the effect of adding compatible left eye gratings) and Experiment 4 (the effect of adding incompatible left eye gratings) as a function of the contrast of the right eye gratings. The failure of additivity as a function of contrast was similar in all three visual areas, although the average suppression of incompatible gratings (Experiment 4) appeared to be more pronounced at high contrasts in V2 and V3 than in V1. A similar trend was found in Experiment 5, in which we directly compared monocular and binocular gratings with monocular and dichoptic plaids (Figure 9B). A three-way ANOVA (observer × condition × visual area) showed a significant effect of condition ($F(3,30) = 7.21$, $p = 0.003$) and a marginally significant effect of visual area ($F(2,30) = 4.06$, $p = 0.051$). Dichoptic plaids evoked V1 responses that were significantly larger than the responses to monocular gratings (Figure 9B), whereas the responses to dichoptic plaids in V2 were not robustly larger than the responses to single monocular gratings. The interaction between visual area and condition, however, was not significant ($F(6,30) = 1.47$, $p = 0.22$).

The overall similarity in the response profile of V2 and V3 to the profile of V1 is compatible with the hypothesis that the normalization in V2 and V3 may be inherited from V1. The slight differences between areas might be attributable to measurement noise (the responses in V2 and V3 were more variable than those in V1) rather than to a real difference in normalization mechanisms.

Discussion

We measured activity in early visual cortex (V1, V2, and V3) elicited by stimulating one eye vs. both eyes, while trying to minimize top-down attentional modulation of the stimulus-evoked responses. The findings can be summarized as follows:

1. If the stimulus contrast was low, then stimulating both eyes with compatible stimuli evoked a larger response than stimulating only one eye.
2. If the stimulus contrast was high, there was little difference in activity evoked by stimulating one eye vs. both eyes.
3. The response to two incompatible stimuli was larger than that evoked by a single stimulus, regardless of whether the two stimuli were superimposed and presented to just one eye or one stimulus was presented to each eye.
4. Additivity (assessed by measuring the response to binocular minus monocular stimulation), for both compatible and incompatible stimuli, depended on contrast, and the failure of additivity was more pronounced as contrast increased.

5. The failure of additivity was greater for stimuli that had the same orientation (additivity index of around zero for high-contrast stimuli) than for orthogonal stimuli (additivity index of around 0.5 for the same contrast level).

The implications of these findings are two-fold. First, our results clearly demonstrate the existence of suppressive inter-ocular interactions in visual cortex. This was evident in V1, V2, and V3, but the suppression in V2 and V3 may very well have been inherited from that in V1. The suppression between the two eyes was comparable to the suppression within one eye. Second, our results suggest that these suppressive inter-ocular interactions are stronger within channels tuned to the same orientation than orthogonal orientations (i.e., comprising a plaid), although there was some suppression for orthogonal orientations as well.

Inter-ocular suppression

Inter-ocular suppression occurs when the response to simultaneous stimulation of both eyes is less than the sum of the responses when each eye is stimulated individually. In other words, a failure of additivity, and particularly a failure that can not be explained by a static nonlinearity (e.g., Equation 9), indicates that activity evoked by one eye somehow suppresses the activity evoked by the other eye and vice versa. Inter-ocular suppression can occur in two contexts. First, it can occur between stimuli that are compatible. Such suppression presumably enables one to experience similar percepts when viewing with either one or both eyes. Second, suppression can occur between incompatible stimuli. In this context, suppression might enable us to resolve incompatibility by blocking one stimulus from perception.

Both types (between compatible stimuli and between incompatible stimuli) require inhibitory inter-ocular interactions. A novel aspect of our study is that we examined inter-ocular suppression (failure of additivity) in both contexts.

Previous psychophysical studies have shown that a discrepancy in contrast between two compatible images could degrade stereopsis (Cormack, Stevenson, & Landers, 1997; Halpern & Blake, 1988; Schor & Heckmann, 1989). That is, inter-ocular interactions that occur within the same orientation channel (but between different contrast levels) could affect performance. Our results indicate that such interactions might also occur when the stimuli have the same contrast.

One previous study (Tse, Martinez-Conde, Schlegel, & Macknik, 2005) reported little evidence of inter-ocular suppression between high-contrast target and mask stimuli in V1. Mask and target presentations alternated in different eyes (dichoptic masking). Target visibility was manipulated by introducing a delay between alternations.

V1 responses did not decrease when the target was made invisible compared to when it was visible. However, when the two stimuli were presented to the same eye, there was suppression of V1 activity associated with masking. Consequently, Tse et al. (2005) concluded that while monocular interactions underlying masking occur in V1, inter-ocular interactions occur only later in the visual pathways.

There were three important differences between our study and that of Tse et al. (2005). First, they presented the target and mask stimuli in alternation and, hence, did not assess inter-ocular interactions between simultaneously presented stimuli. Second, the mask and target were incompatible, and hence the study did not assess inter-ocular interactions between compatible stimuli. Third, their results should not be interpreted as evidence of the absence of inter-ocular interactions. Rather, they simply showed that interactions in their particular case did not correlate with visibility. Our experimental protocols allowed us to establish that inter-ocular suppression affects the activity in primary visual cortex. We found almost complete suppression of compatible gratings (Experiment 2) and about 50% suppression for incompatible gratings (dichoptic plaid, Experiments 4–6), with contrasts of 10% or higher.

Our results might seem at odds with single cell recordings that suggest contrast normalization and cross-orientation suppression are mainly monocular (Truchard et al., 2000; Walker et al., 1998). Walker et al. (1998) reported that although inter-ocular suppression for orthogonal stimuli was present in almost all cells they recorded, such effects were generally weak. Based on this, we might have expected more suppression and smaller fMRI responses to monocular plaids than to dichoptic plaids. However, that is not what we observed (Figure 7).

On the other hand, phenomenal suppression is stronger between the eyes (binocular rivalry) than within one eye (monocular rivalry; Andrews & Purves, 1997; Sindermann & Lüddeke, 1972; Wade, 1975). Based on this, we might have expected more suppression and smaller fMRI responses to dichoptic plaids than to monocular plaids. However, we did not observe this either (Figures 7 and 8), as discussed further in the following section. Thus, the fMRI results were qualitatively between what happens at the single neuron level and at the perceptual level. More studies are necessary to reconcile these differences and elucidate the effects of different stimulus properties and experimental protocols, along with the role of top-down influences (such as attention), on inter-ocular suppression.

Binocular rivalry and flash suppression

Binocular rivalry occurs when viewing a dichoptic plaid for an extended period of time; one of the two gratings becomes perceptually dominant while the other grating is perceptually suppressed, and the dominant and suppressed gratings alternate over time. However, if two incompatible gratings are superimposed and presented to the same eye (monocular plaid), rivalry and suppression are negligible or, at best, substantially weaker (Campbell & Howell, 1972; Sindermann & Lüddeke, 1972; Wade, 1975). Several previous fMRI studies have reported modulations in V1 activity concomitant with the perceptual alternations during binocular rivalry (Haynes & Rees, 2005a, 2005b; Lee, Blake, & Heeger, 2005, 2007; Polonsky, Blake, Braun, & Heeger, 2000; Tong & Engel, 2001; Wunderlich, Schneider, & Kastner, 2005). In some (but not all) of these studies, the amplitudes of the activity modulations during rivalry were nearly the same as those resulting from turning the stimuli physically on and off. This has been taken as evidence that V1 activity corresponding to one or the other stimulus was completely suppressed.

Our results were not consistent with this conclusion. Quite the opposite: To our surprise, the suppression for incompatible stimuli (dichoptic plaids) was only half of that observed for compatible stimuli (binocular gratings), and the responses to dichoptic plaids were significantly larger than the responses to monocular gratings. The input from the "would have been suppressed eye" (if observers were seeing the gratings) reached V1 and increased the V1 responses. Although our results showed suppression between orthogonal stimuli, the suppression was weaker (about half of the activity evoked by each eye's stimulus in isolation) than that from compatible (same orientation) stimuli and did not depend on the eye of origin.

This lack of complete suppression was consistent with a number of previously published results. Some of the human fMRI studies of rivalry have reported a lack of complete suppression (Lee et al., 2005, 2007; Polonsky et al., 2000). The responses of only a subpopulation of V1 neurons recorded electrophysiologically have been found to correlate with perceptual fluctuations during rivalry (Leopold & Logothetis, 1996). In addition, a number of psychophysical observations suggest that the neural events underlying phenomenal suppression of a stimulus are not the same as those accompanying physical removal of that stimulus (Alais & Parker, 2006; Andrews & Blakemore, 1999; Blake & Camisa, 1979; Blake & Fox, 1974; Blake & Overton, 1979; Blake, Tadin, Sobel, Raissian, & Chong, 2006; Lehmkuhle & Fox, 1975; Nguyen, Freeman, & Alais, 2003; O'Shea, 1987; O'Shea & Crassini, 1981; Smith, Levi, Harwerth, & White, 1982; Wade, 1976; Wiesenfelder & Blake, 1991).

One caveat concerning our experimental protocol is that the observers' attention was focused on the central task, so there was, by design, no access to the observers' percepts of the gratings. For most of the experimental conditions, we do not know if subjects would have experienced complete suppression of one of the two gratings, patchy rivalry/suppression, or fusion. The two incompatible gratings, when presented simultaneously, might have required more time to develop stronger suppression

leading to rivalry. One of the goals of Experiment 6 was to circumvent this ambiguity by using a flash suppression protocol to control the dynamics of phenomenal suppression. However, we still found inter-ocular suppression roughly equal to monocular cross-orientation suppression. That is, there was no evidence for the additional suppression that would be needed to account for the perceptual phenomenon of flash suppression. Hence, our results suggest that most, if not all, of the suppression could be attributed to general cross-orientation suppression (independent of eye of origin). A similar conclusion has been reached using visual evoked potentials (Lennerstrand, 1978).

Might differences in the observer's attention state (i.e., whether or not the observer was monitoring the perception of the incompatible stimuli) contribute to why our results differed from previous studies showing almost complete suppression of the responses to one of two incompatible stimuli? Psychophysical (Chong & Blake, 2006; Chong, Tadin, & Blake, 2005; Hancock & Andrews, 2007; Kanai, Moradi, Shimojo, & Verstraten, 2005; Mitchell, Stoner, & Reynolds, 2004; Ooi & He, 1999; Sasaki & Gyoba, 2002), pharmacological (Carter et al., 2007), and brain imaging (Lee et al., 2007; Lumer, Friston, & Rees, 1998) studies all suggest a link between rivalry and attention. Could it be that response modulations in V1 (or the LGN) correlating with observers' percepts during binocular rivalry (or flash suppression) are evident only when observers attend the incompatible stimuli? Competition and neural suppression corresponding to phenomenal awareness might originate in V1 or earlier (LGN) during normal viewing but might be turned off when attention is diverted.

Only one previous study (Lee et al., 2007) examined binocular rivalry with a diversion of attention comparable to that in the current experiments. During transitions in perceptual state, one typically perceives a traveling wave in which the perceptual dominance of one pattern emerges locally and expands progressively as it renders the other pattern invisible (Wilson, Blake, & Lee, 2001). Lee et al. (2007) measured traveling waves of cortical activity propagating over subregions of V1 that corresponded topographically to perceptual waves, both when observers were attending and perceiving the waves and when their attention was diverted. Their traveling wave protocol utilized similar stimuli (dichoptic plaids made of spiral gratings, same eccentricity and spatial frequency) and the same experimental setup. However, we failed to find any evidence in the current experiments that inter-ocular suppression (with a dichoptic plaid) was stronger than monocular suppression (monocular plaid), even with a temporal delay between the onsets of incompatible stimuli presented to the two eyes, which, under normal viewing conditions, results in flash suppression. How can we reconcile these ostensibly contradictory results? One possibility is that the traveling waves of activity in V1 in the absence of attention, reported by Lee et al., reflect cross-orientation suppression rather than binocular rivalry. This could be tested by repeating the traveling wave

experiments with monocular stimulation. A second possibility is that the mechanism of inter-ocular suppression underlying the traveling waves during rivalry is different from that underlying flash suppression. The traveling wave protocol utilized both flash suppression and a spatially localized and transient contrast increment to induce perceptual transitions; the combination of the two might lead to stronger suppression even when attention is diverted. A third possibility is that the traveling wave could reflect the emerging dominance of the grating that becomes visible rather than the suppression of the competing grating; perceptual dominance and suppression may not strictly be two sides of the same coin (Blake & Logothetis, 2002).

Normalization of visual responses

The contrast normalization model provided a quantitative explanation for the responses to pairs of compatible and incompatible gratings presented monocularly and dichoptically. For compatible stimuli, we assumed that both eyes contributed equally to the normalization term. However, for incompatible stimuli (monocular plaids and dichoptic plaids), the best fit was obtained when orthogonal orientations contributed only about half as much suppression as compatible orientations. The nonlinear binocular summation model (Equation 5) and the binocular normalization model (Equation 6) provided comparable fits to the data. Even so, we prefer the binocular normalization model because the nonlinear binocular summation model assumes that all cortical neurons are binocular, with no contribution from monocular neurons to the pooled activity as measured with fMRI. In contrast, a model that assumed monocular normalization followed by linear binocular summation did not fit the data.

The binocular contrast normalization model that we used to fit our fMRI data is comparable to models inferred from psychophysical studies of binocular summation (Arditi, Anderson, & Movshon, 1981; Baker et al., 2007; Ding & Sperling, 2006; Legge, 1984; Meese, Georgeson, & Baker, 2006). These models, some of which are conceptually very similar to our model whereas others are more complex, have been proposed to account for psychophysical measurements of contrast discrimination, for the improved performance in binocular vs. monocular viewing, and for the effect of dichoptic masks. Virtually all these models incorporate binocular normalization as opposed to monocular normalization followed by binocular linear summation.

There are some differences between our simple model and more sophisticated models that are needed to explain behavioral results. For example, not all of the psychophysical models predict sublinear responses for contrast levels larger than 10%, as was observed in our fMRI measurements. As another example, the model suggested by Ding and Sperling (2006) predicts that the response to

a 10% contrast grating in one eye and a 50% contrast grating in the other eye should be smaller than the response to the 50% contrast grating presented monocularly (i.e., the additivity index would be negative). The normalization model described in Equation 6 predicts the opposite (the additivity index is a small but positive number). The quantitative difference in activity between these models, however, is too small (a few percent) to be resolved by our fMRI data.

Early saturation of monocular contrast response function

Our measurements of the V1 contrast response function began to saturate (reach a plateau) at ∼10% contrast, that is, at a lower contrast than that reported in some previous fMRI studies and lower than that inferred from some previous psychophysical studies. Saturation at such low contrasts is commonly reported in single-unit electrophysiology and visual-evoked potential studies (Albrecht & Hamilton, 1982; Carandini et al., 1997; Geisler & Albrecht, 1997; Park, Zhang, Ferrera, Hirsch, & Hood, 2008). Another fMRI study (Li, Lu, Tjan, Dosher, & Chu, 2008) that used an event-related design also found contrast response curves that, similar to our current study, were steeper and saturated earlier than those reported in studies that used a block-alternation design (Boynton et al., 1999; Olman, Ugurbil, Schrater, & Kersten, 2004; Zenger-Landolt & Heeger, 2003). The difference in shape of contrast response curves could be attributed to differences in stimulation (stationary stimuli vs. contrast reversing at 8 Hz), duration of stimulation and adaptation (1.5 s vs. 18 s; Gardner et al., 2005), or (although less likely, cf. Murray & He, 2006) attention. This might seem at odds with previous studies reporting fMRI responses that were consistent with psychophysical contrast discrimination curves (Boynton et al., 1999; Zenger-Landolt & Heeger, 2003). However, the earlier studies demonstrating a match between fMRI and psychophysics did so using the same protocol for both sets of measurements, so that these stimulation, attention and/or adaptation factors would have had the same effect on both the psychophysics and the fMRI, thereby leaving the comparison between them valid.

Neural mechanisms underlying normalization

Although contrast gain control has been shown to be evident in the retina and LGN, our results imply a cortical mechanism for binocular normalization. The inputs from the eyes are separate before reaching V1, and inter-ocular interactions in earlier stages are unlikely. We found that normalization depended on the similarity between the orientations of the stimuli presented to the eyes. Unlike V1 neurons, LGN neurons are not orientation selective so normalization at a level before V1 cannot explain why normalization between gratings with the same orientation was stronger than normalization between orthogonal gratings.

The complete failure of additivity for high-contrast stimuli with the same orientation suggests that the inter-ocular suppression in V1 is ubiquitous. Inputs from the two eyes are, to some extent, segregated in V1 and this can be visualized with fMRI (Buchert et al., 2002; Cheng, Waggoner, & Tanaka, 2001; Haynes & Rees, 2005a, 2005b; Menon, Ogawa, Strupp, & Uğurbil, 1997). The responses of purely monocular neurons, i.e., neurons unaffected by stimulation of the other eye (whether it is within or outside of their classical receptive field), would by definition exhibit responses that are independent of the contrast of the other eye. We thus expected to find residual additivity for high-contrast stimuli reflecting the activity of purely monocular neurons. However, the additivity reached zero as the contrast of the other eye increased to 10% or more.

A similar argument can be made concerning the suppressive interaction between orthogonal stimuli. If orthogonal orientation channels were independent of each other, then a dichoptic plaid would have evoked twice the activity evoked by a single grating. However, for high-contrast stimuli, the overall fMRI response to a plaid was considerably smaller (by 50% or more) than the linear summation of responses to the plaid's grating components.

Our results suggest that monocular synaptic inputs from LGN neurons are not dominant in fMRI measurements of V1 activity. It has been suggested that cortical oxygen concentration (and by inference, fMRI responses) reflects primarily input synaptic activity (Viswanathan & Freeman, 2007). A similar conclusion has been made based on comparisons between electrophysiological and fMRI measurements (Goense & Logothetis, 2008; Logothetis, Pauls, Augath, Trinath, & Oeltermann, 2001), and based on fMRI measurements while pharmacologically blocking cortical spiking activity (Rauch, Rainer, & Logothetis, 2008). If fMRI responses were dominated by synaptic inputs from the LGN, however, then the linear binocular summation and/or the power-law model would have fit the data well. The strong inter-ocular and cross-orientation suppression evident in our data implies just the opposite, that the fMRI measurements are dominated by the activity of cortical neurons.

Overall, our results suggest that the activity in V1 is highly regulated by suppressive mechanisms that prevent excessive excitation in response to doubling the input. Normalization was able to explain quantitatively these suppressive interactions, as measured by fMRI. Our results are consistent with the idea that divisive normalization is ubiquitous in visual cortex and plays an important role in computations that underlie visual processing.

Acknowledgments

Commercial relationships: none.
Corresponding author: Farshad Moradi.
Email: farshadm@caltech.edu.
Address: 139-74 California Institute of Technology, 1200 E California Blvd., Pasadena, CA 91125, USA.

References

Alais, D., & Parker, A. (2006). Independent binocular rivalry processes for motion and form. *Neuron, 52,* 911–920. [PubMed] [Article]

Albrecht, D. G., & Geisler, W. S. (1991). Motion selectivity and the contrast-response function of simple cells in the visual cortex. *Visual Neuroscience, 7,* 531–546. [PubMed]

Albrecht, D. G., & Hamilton, D. B. (1982). Striate cortex of monkey and cat: Contrast response function. *Journal of Neurophysiology, 48,* 217–237. [PubMed]

Allman, J., Miezin, F., & McGuinness, E. (1985). Direction- and velocity-specific responses from beyond the classical receptive field in the middle temporal visual area (MT). *Perception, 14,* 105–126. [PubMed]

Andrews, T. J., & Blakemore, C. (1999). Form and motion have independent access to consciousness. *Nature Neuroscience, 2,* 405–406. [PubMed]

Andrews, T. J., & Purves, D. (1997). Similarities in normal and binocularly rivalrous viewing. *Proceedings of the National Academy of Sciences of the United States of America, 94,* 9905–9908. [PubMed] [Article]

Arditi, A. R., Anderson, P. A., & Movshon, J. A. (1981). Monocular and binocular detection of moving sinusoidal gratings. *Vision Research, 21,* 329–336. [PubMed]

Baccus, S. A., & Meister, M. (2002). Fast and slow contrast adaptation in retinal circuitry. *Neuron, 36,* 909–919. [PubMed] [Article]

Bair, W., Cavanaugh, J. R., & Movshon, J. A. (2003). Time course and time–distance relationships for surround suppression in macaque V1 neurons. *Journal of Neuroscience, 23,* 7690–7701. [PubMed] [Article]

Baker, D. H., Meese, T. S., & Georgeson, M. A. (2007). Binocular interaction: Contrast matching and contrast discrimination are predicted by the same model. *Spatial Vision, 20,* 397–413. [PubMed]

Bauman, L. A., & Bonds, A. B. (1991). Inhibitory refinement of spatial frequency selectivity in single cells of the cat striate cortex. *Vision Research, 31,* 933–944. [PubMed]

Bearse, M. A., Jr., & Freeman, R. D. (1994). Binocular summation in orientation discrimination depends on stimulus contrast and duration. *Vision Research, 34,* 19–29. [PubMed]

Blake, R., & Camisa, J. (1979). On the inhibitory nature of binocular rivalry suppression. *Journal of Experimental Psychology: Human Perception and Performance, 5,* 315–323. [PubMed]

Blake, R., & Fox, R. (1974). Adaptation to invisible gratings and the site of binocular rivalry suppression. *Nature, 249,* 488–490. [PubMed]

Blake, R., & Logothetis, N. K. (2002). Visual competition. *Nature Reviews, Neuroscience, 3,* 13–21. [PubMed]

Blake, R., & Overton, R. (1979). The site of binocular rivalry suppression. *Perception, 8,* 143–152. [PubMed]

Blake, R., Tadin, D., Sobel, K. V., Raissian, T. A., & Chong, S. C. (2006). Strength of early visual adaptation depends on visual awareness. *Proceedings of the National Academy of Sciences of the United States of America, 103,* 4783–4788. [PubMed] [Article]

Blakemore, C., & Tobin, E. A. (1972). Lateral inhibition between orientation detectors in the cat's visual cortex. *Experimental Brain Research, 15,* 439–440. [PubMed]

Bonds, A. B. (1989). Role of inhibition in the specification of orientation selectivity of cells in the cat striate cortex. *Visual Neuroscience, 2,* 41–55. [PubMed]

Bonin, V., Mante, V., & Carandini, M. (2005). The suppressive field of neurons in lateral geniculate nucleus. *Journal of Neuroscience, 25,* 10844–10856. [PubMed] [Article]

Boynton, G. M., Demb, J. B., Glover, G. H., & Heeger, D. J. (1999). Neuronal basis of contrast discrimination. *Vision Research, 39,* 257–269. [PubMed]

Boynton, G. M., Engel, S. A., Glover, G. H., & Heeger, D. J. (1996). Linear systems analysis of functional magnetic resonance imaging in human V1. *Journal of Neuroscience, 16,* 4207–4221. [PubMed] [Article]

Boynton, G. M., & Foley, J. M. (1999). Temporal sensitivity of human luminance pattern mechanisms determined by masking with temporally modulated stimuli. *Vision Research, 39,* 1641–1656. [PubMed]

Britten, K. H., & Heuer, H. W. (1999). Spatial summation in the receptive fields of MT neurons. *Journal of Neuroscience, 19,* 5074–5084. [PubMed] [Article]

Buchert, M., Greenlee, M. W., Rutschmann, R. M., Kraemer, F. M., Luo, F., & Hennig, J. (2002). Functional magnetic resonance imaging evidence for binocular interactions in human visual cortex. *Experimental Brain Research, 145,* 334–339. [PubMed]

Buracas, G. T., & Boynton, G. M. (2002). Efficient design of event-related fMRI experiments using M-sequences. *Neuroimage, 16,* 801–813. [PubMed]

Burr, D. C., & Morrone, M. C. (1987). Inhibitory interactions in the human vision system revealed in pattern-evoked potentials. *The Journal of Physiology, 389,* 1–21. [PubMed] [Article]

Cagenello, R., Arditi, A., & Halpern, D. L. (1993). Binocular enhancement of visual acuity. *Journal of the Optical Society of America A, Optics, Image Science, and Vision, 10,* 1841–1848. [PubMed]

Campbell, F. W., & Howell, E. R. (1972). Monocular alternation: A method for the investigation of pattern vision. *The Journal of Physiology, 225,* 19P–21P. [PubMed]

Candy, T. R., Skoczenski, A. M., & Norcia, A. M. (2001). Normalization models applied to orientation masking in the human infant. *Journal of Neuroscience, 21,* 4530–4541. [PubMed] [Article]

Carandini, M., & Heeger, D. J. (1994). Summation and division by neurons in primate visual cortex. *Science, 264,* 1333–1336. [PubMed]

Carandini, M., Heeger, D. J., & Movshon, J. A. (1997). Linearity and normalization in simple cells of the macaque primary visual cortex. *Journal of Neuroscience, 17,* 8621–8644. [PubMed] [Article]

Carter, O. L., Hasler, F., Pettigrew, J. D., Wallis, G. M., Liu, G. B., & Vollenweider, F. X. (2007). Psilocybin links binocular rivalry switch rate to attention and subjective arousal levels in humans. *Psychopharmacology, 195,* 415–424. [PubMed]

Cavanaugh, J. R., Bair, W., & Movshon, J. A. (2002a). Nature and interaction of signals from the receptive field center and surround in macaque V1 neurons. *Journal of Neurophysiology, 88,* 2530–2546. [PubMed] [Article]

Cavanaugh, J. R., Bair, W., & Movshon, J. A. (2002b). Selectivity and spatial distribution of signals from the receptive field surround in macaque V1 neurons. *Journal of Neurophysiology, 88,* 2547–2556. [PubMed] [Article]

Cheng, K., Waggoner, R. A., & Tanaka, K. (2001). Human ocular dominance columns as revealed by high-field functional magnetic resonance imaging. *Neuron, 32,* 359–374. [PubMed] [Article]

Chong, S. C., & Blake, R. (2006). Exogenous attention and endogenous attention influence initial dominance in binocular rivalry. *Vision Research, 46,* 1794–1803. [PubMed]

Chong, S. C., Tadin, D., & Blake, R. (2005). Endogenous attention prolongs dominance durations in binocular rivalry. *Journal of Vision, 5*(11):6, 1004–1012, http://journalofvision.org/5/11/6/, doi:10.1167/5.11.6. [PubMed] [Article]

Cormack, L. K., Stevenson, S. B., & Landers, D. D. (1997). Interactions of spatial frequency and unequal monocular contrasts in stereopsis. *Perception, 26,* 1121–1136. [PubMed]

Dale, A. M. (1999). Optimal experimental design for event-related fMRI. *Human Brain Mapping, 8,* 109–114. [PubMed]

DeAngelis, G. C., Freeman, R. D., & Ohzawa, I. (1994). Length and width tuning of neurons in the cat's primary visual cortex. *Journal of Neurophysiology, 71,* 347–374. [PubMed]

DeYoe, E. A., Carman, G. J., Bandettini, P., Glickman, S., Wieser, J., Cox, R., et al. (1996). Mapping striate and extrastriate visual areas in human cerebral cortex. *Proceedings of the National Academy of Sciences of the United States of America, 93,* 2382–2386. [PubMed] [Article]

Ding, J., & Sperling, G. (2006). A gain-control theory of binocular combination. *Proceedings of the National Academy of Sciences of the United States of America, 103,* 1141–1146. [PubMed] [Article]

Engel, S. A., Glover, G. H., & Wandell, B. A. (1997). Retinotopic organization in human visual cortex and the spatial precision of functional MRI. *Cerebral Cortex, 7,* 181–192. [PubMed] [Article]

Engel, S. A., Rumelhart, D. E., Wandell, B. A., Lee, A. T., Glover, G. H., Chichilnisky, E. J., et al. (1994). fMRI of human visual cortex. *Nature, 369,* 525. [PubMed]

Foley, J. M. (1994). Human luminance pattern-vision mechanisms: Masking experiments require a new model. *Journal of the Optical Society of America A, Optics, Image Science, and Vision, 11,* 1710–1719. [PubMed]

Foley, J. M., & Chen, C. C. (1997). Analysis of the effect of pattern adaptation on pattern pedestal effects: A two-process model. *Vision Research, 37,* 2779–2788. [PubMed]

Gardner, J. L., Sun, P., Waggoner, R. A., Ueno, K., Tanaka, K., & Cheng, K. (2005). Contrast adaptation and representation in human early visual cortex. *Neuron, 47,* 607–620. [PubMed] [Article]

Geisler, W. S., & Albrecht, D. G. (1997). Visual cortex neurons in monkeys and cats: Detection, discrimination, and identification. *Visual Neuroscience, 14,* 897–919. [PubMed]

Goense, J. B., & Logothetis, N. K. (2008). Neurophysiology of the BOLD fMRI signal in awake monkeys. *Current Biology, 18,* 631–640. [PubMed]

Grossberg, S. (1973). Contour enhancement, short term memory, and constancies in reverberating neural networks. *Studies in Applied Mathematics, 52,* 213–257.

Halpern, D. L., & Blake, R. R. (1988). How contrast affects stereoacuity. *Perception, 17,* 483–495. [PubMed]

Hancock, S., & Andrews, T. J. (2007). The role of voluntary and involuntary attention in selecting perceptual dominance during binocular rivalry. *Perception, 36,* 288–298. [PubMed]

Haynes, J. D., & Rees, G. (2005a). Predicting the orientation of invisible stimuli from activity in human primary visual cortex. *Nature Neuroscience, 8,* 686–691. [PubMed]

Haynes, J. D., & Rees, G. (2005b). Predicting the stream of consciousness from activity in human visual cortex. *Current Biology, 15,* 1301–1307. [PubMed] [Article]

Heeger, D. J. (1991). Nonlinear model of neural responses in cat visual cortex. In M. S. Landy & J. A. Movshon (Eds.), *Computational models of visual processing* (pp. 119–133). Cambridge, MA: MIT Press.

Heeger, D. J. (1992a). Half-squaring in responses of cat striate cells. *Visual Neuroscience, 9,* 427–443. [PubMed]

Heeger, D. J. (1992b). Normalization of cell responses in cat striate cortex. *Visual Neuroscience, 9,* 181–197. [PubMed]

Heeger, D. J. (1993). Modeling simple-cell direction selectivity with normalized, half-squared, linear operators. *Journal of Neurophysiology, 70,* 1885–1898. [PubMed]

Heeger, D. J., Simoncelli, E. P., & Movshon, J. A. (1996). Computational models of cortical visual processing. *Proceedings of the National Academy of Sciences of the United States of America, 93,* 623–627. [PubMed] [Article]

Jenkinson, M., Bannister, P., Brady, M., & Smith, S. (2002). Improved optimization for the robust and accurate linear registration and motion correction of brain images. *Neuroimage, 17,* 825–841. [PubMed]

Kamitani, Y., & Tong, F. (2005). Decoding the visual and subjective contents of the human brain. *Nature Neuroscience, 8,* 679–685. [PubMed] [Article]

Kanai, R., Moradi, F., Shimojo, S., & Verstraten, F. A. (2005). Perceptual alternation induced by visual transients. *Perception, 34,* 803–822. [PubMed]

Kaplan, E., Purpura, K., & Shapley, R. M. (1987). Contrast affects the transmission of visual information through the mammalian lateral geniculate nucleus. *The Journal of Physiology, 391,* 267–288. [PubMed] [Article]

Kouh, M., & Poggio, T. (2008). A canonical neural circuit for cortical nonlinear operations. *Neural Computation, 20,* 1427–1451. [PubMed]

Lee, S. H., Blake, R., & Heeger, D. J. (2005). Traveling waves of activity in primary visual cortex during binocular rivalry. *Nature Neuroscience, 8,* 22–23. [PubMed] [Article]

Lee, S. H., Blake, R., & Heeger, D. J. (2007). Hierarchy of cortical responses underlying binocular rivalry. *Nature Neuroscience, 10,* 1048–1054. [PubMed] [Article]

Legge, G. E. (1984). Binocular contrast summation—I. Detection and discrimination. *Vision Research, 24,* 373–383. [PubMed]

Lehmkuhle, S. W., & Fox, R. (1975). Effect of binocular rivalry suppression on the motion aftereffect. *Vision Research, 15,* 855–859. [PubMed]

Lennerstrand, G. (1978). Some observations on visual evoked responses (VER) to dichoptic stimulation. *Acta Ophthalmologica, 56,* 638–647. [PubMed]

Leopold, D. A., & Logothetis, N. K. (1996). Activity changes in early visual cortex reflect monkeys' percepts during binocular rivalry. *Nature, 379,* 549–553. [PubMed]

Levitt, J. B., & Lund, J. S. (1997). Contrast dependence of contextual effects in primate visual cortex. *Nature, 387,* 73–76. [PubMed]

Li, X., Lu, Z. L., Tjan, B. S., Dosher, B. A., & Chu, W. (2008). Blood oxygenation level-dependent contrast response functions identify mechanisms of covert attention in early visual areas. *Proceedings of the National Academy of Sciences of the United States of America, 105,* 6202–6207. [PubMed] [Article]

Logothetis, N. K., Pauls, J., Augath, M., Trinath, T., & Oeltermann, A. (2001). Neurophysiological investigation of the basis of the fMRI signal. *Nature, 412,* 150–157. [PubMed]

Lumer, E. D., Friston, K. J., & Rees, G. (1998). Neural correlates of perceptual rivalry in the human brain. *Science, 280,* 1930–1934. [PubMed]

Mante, V., Frazor, R. A., Bonin, V., Geisler, W. S., & Carandini, M. (2005). Independence of luminance and contrast in natural scenes and in the early visual system. *Nature Neuroscience, 8,* 1690–1697. [PubMed]

Meese, T. S., Georgeson, M. A., & Baker, D. H. (2006). Binocular contrast vision at and above threshold. *Journal of Vision, 6*(11):7, 1224–1243, http://journalofvision.org/6/11/7/, doi:10.1167/6.11.7. [PubMed] [Article]

Meese, T. S., & Holmes, D. J. (2002). Adaptation and gain pool summation: Alternative models and masking data. *Vision Research, 42,* 1113–1125. [PubMed]

Menon, R. S., Ogawa, S., Strupp, J. P., & Uğurbil, K. (1997). Ocular dominance in human V1 demonstrated

by functional magnetic resonance imaging. *Journal of Neurophysiology, 77,* 2780–2787. [PubMed] [Article]

Miller, E. K., Gochin, P. M., & Gross, C. G. (1993). Suppression of visual responses of neurons in inferior temporal cortex of the awake macaque by addition of a second stimulus. *Brain Research, 616,* 25–29. [PubMed]

Missal, M., Vogels, R., & Orban, G. A. (1997). Responses of macaque inferior temporal neurons to overlapping shapes. *Cerebral Cortex, 7,* 758–767. [PubMed] [Article]

Mitchell, J. F., Stoner, G. R., & Reynolds, J. H. (2004). Object-based attention determines dominance in binocular rivalry. *Nature, 429,* 410–413. [PubMed]

Morrone, M. C., Burr, D. C., & Maffei, L. (1982). Functional implications of cross-orientation inhibition of cortical visual cells. I. Neurophysiological evidence. *Proceedings of the Royal Society of London B: Biological Sciences, 216,* 335–354. [PubMed]

Murray, S. O., & He, S. (2006). Contrast invariance in the human lateral occipital complex depends on attention. *Current Biology, 16,* 606–611. [PubMed] [Article]

Nelson, J. I., & Frost, B. J. (1985). Intracortical facilitation among co-oriented, co-axially aligned simple cells in cat striate cortex. *Experimental Brain Research, 61,* 54–61. [PubMed]

Nestares, O., & Heeger, D. J. (1997). Modeling the apparent frequency-specific suppression in simple cell responses. *Vision Research, 37,* 1535–1543. [PubMed]

Nestares, O., & Heeger, D. J. (2000). Robust multi-resolution alignment of MRI brain volumes. *Magnetic Resonance in Medicine, 43,* 705–715. [PubMed]

Nguyen, V. A., Freeman, A. W., & Alais, D. (2003). Increasing depth of binocular rivalry suppression along two visual pathways. *Vision Research, 43,* 2003–2008. [PubMed]

Olman, C. A., Ugurbil, K., Schrater, P., & Kersten, D. (2004). BOLD fMRI and psychophysical measurements of contrast response to broadband images. *Vision Research, 44,* 669–683. [PubMed]

Ooi, T. L., & He, Z. J. (1999). Binocular rivalry and visual awareness: The role of attention. *Perception, 28,* 551–574. [PubMed]

O'Shea, R. P. (1987). Chronometric analysis supports fusion rather than suppression theory of binocular vision. *Vision Research, 27,* 781–791. [PubMed]

O'Shea, R. P., & Crassini, B. (1981). Interocular transfer of the motion after-effect is not reduced by binocular rivalry. *Vision Research, 21,* 801–804. [PubMed]

Park, J. C., Zhang, X., Ferrera, J., Hirsch, J., & Hood, D. C. (2008). Comparison of contrast-response functions from multifocal visual-evoked potentials (mfVEPs) and functional MRI responses. *Journal of Vision, 8*(10):8, 1–12, http://journalofvision.org/8/10/8/, doi:10.1167/8.10.8. [PubMed] [Article]

Polonsky, A., Blake, R., Braun, J., & Heeger, D. J. (2000). Neuronal activity in human primary visual cortex correlates with perception during binocular rivalry. *Nature Neuroscience, 3,* 1153–1159. [PubMed]

Rauch, A., Rainer, G., & Logothetis, N. K. (2008). The effect of a serotonin-induced dissociation between spiking and perisynaptic activity on BOLD functional MRI. *Proceedings of the National Academy of Sciences of the United States of America, 105,* 6759–6764. [PubMed] [Article]

Recanzone, G. H., Wurtz, R. H., & Schwarz, U. (1997). Responses of MT and MST neurons to one and two moving objects in the receptive field. *Journal of Neurophysiology, 78,* 2904–2915. [PubMed] [Article]

Reynolds, J. H., Chelazzi, L., & Desimone, R. (1999). Competitive mechanisms subserve attention in macaque areas V2 and V4. *Journal of Neuroscience, 19,* 1736–1753. [PubMed] [Article]

Richmond, B. J., Wurtz, R. H., & Sato, T. (1983). Visual responses of inferior temporal neurons in awake rhesus monkey. *Journal of Neurophysiology, 50,* 1415–1432. [PubMed]

Rolls, E. T., & Tovee, M. J. (1995). The responses of single neurons in the temporal visual cortical areas of the macaque when more than one stimulus is present in the receptive field. *Experimental Brain Research, 103,* 409–420. [PubMed]

Sasaki, H., & Gyoba, J. (2002). Selective attention to stimulus features modulates interocular suppression. *Perception, 31,* 409–419. [PubMed]

Sato, T. (1989). Interactions of visual stimuli in the receptive fields of inferior temporal neurons in awake macaques. *Experimental Brain Research, 77,* 23–30. [PubMed]

Schor, C., & Heckmann, T. (1989). Interocular differences in contrast and spatial frequency: Effects on stereopsis and fusion. *Vision Research, 29,* 837–847. [PubMed]

Sereno, M. I., Dale, A. M., Reppas, J. B., Kwong, K. K., Belliveau, J. W., Brady, T. J., et al. (1995). Borders of multiple visual areas in humans revealed by functional magnetic resonance imaging. *Science, 268,* 889–893. [PubMed]

Shapley, R. M., & Victor, J. D. (1978). The effect of contrast on the transfer properties of cat retinal ganglion cells. *The Journal of Physiology, 285,* 275–298. [PubMed] [Article]

Shapley, R. M., & Victor, J. D. (1981). How the contrast gain control modifies the frequency responses of cat

retinal ganglion cells. *The Journal of Physiology, 318,* 161–179. [PubMed] [Article]

Simoncelli, E. P., & Heeger, D. J. (1998). A model of neuronal responses in visual area MT. *Vision Research, 38,* 743–761. [PubMed]

Sindermann, F., & Lüddeke, H. (1972). Monocular analogues to binocular contour rivalry. *Vision Research, 12,* 763–772. [PubMed]

Smith, E. L., Levi, D. M., Harwerth, R. S., & White, J. M. (1982). Color vision is altered during the suppression phase of binocular rivalry. *Science, 218,* 802–804. [PubMed]

Snowden, R. J., Treue, S., Erickson, R. G., & Andersen, R. A. (1991). The response of area MT and V1 neurons to transparent motion. *Journal of Neuroscience, 11,* 2768–2785. [PubMed] [Article]

Sperling, G., & Sondhi, M. M. (1968). Model for visual luminance discrimination and flicker detection. *Journal of the Optical Society of America, 58,* 1133–1145. [PubMed]

Tolhurst, D. J., & Heeger, D. J. (1997a). Comparison of contrast-normalization and threshold models of the responses of simple cells in cat striate cortex. *Visual Neuroscience, 14,* 293–309. [PubMed]

Tolhurst, D. J., & Heeger, D. J. (1997b). Contrast normalization and a linear model for the directional selectivity of simple cells in cat striate cortex. *Visual Neuroscience, 14,* 19–25. [PubMed]

Tong, F., & Engel, S. A. (2001). Interocular rivalry revealed in the human cortical blind-spot representation. *Nature, 411,* 195–199. [PubMed]

Treue, S., Hol, K., & Rauber, H. J. (2000). Seeing multiple directions of motion-physiology and psychophysics. *Nature Neuroscience, 3,* 270–276. [PubMed]

Truchard, A. M., Ohzawa, I., & Freeman, R. D. (2000). Contrast gain control in the visual cortex: Monocular versus binocular mechanisms. *Journal of Neuroscience, 20,* 3017–3032. [PubMed] [Article]

Tse, P. U., Martinez-Conde, S., Schlegel, A. A., & Macknik, S. L. (2005). Visibility, visual awareness, and visual masking of simple unattended targets are confined to areas in the occipital cortex beyond human V1/V2. *Proceedings of the National Academy of Sciences of the United States of America, 102,* 17178–17183. [PubMed] [Article]

Viswanathan, A., & Freeman, R. D. (2007). Neuro-metabolic coupling in cerebral cortex reflects synaptic more than spiking activity. *Nature Neuroscience, 10,* 1308–1312. [PubMed]

Wade, N. J. (1975). Monocular and binocular rivalry between contours. *Perception, 4,* 85–95. [PubMed]

Wade, N. J. (1976). On interocular transfer of the movement aftereffect in individuals with and without normal binocular vision. *Perception, 5,* 113–118. [PubMed]

Walker, G. A., Ohzawa, I., & Freeman, R. D. (1998). Binocular cross-orientation suppression in the cat's striate cortex. *Journal of Neurophysiology, 79,* 227–239. [PubMed] [Article]

Wiesenfelder, H., & Blake, R. (1991). Apparent motion can survive binocular rivalry suppression. *Vision Research, 31,* 1589–1599. [PubMed]

Wilson, H. R., Blake, R., & Lee, S. H. (2001). Dynamics of travelling waves in visual perception. *Nature, 412,* 907–910. [PubMed]

Wolfe, J. M. (1984). Reversing ocular dominance and suppression in a single flash. *Vision Research, 24,* 471–478. [PubMed]

Wunderlich, K., Schneider, K. A., & Kastner, S. (2005). Neural correlates of binocular rivalry in the human lateral geniculate nucleus. *Nature Neuroscience, 8,* 1595–1602. [PubMed] [Article]

Zenger-Landolt, B., & Heeger, D. J. (2003). Response suppression in v1 agrees with psychophysics of surround masking. *Journal of Neuroscience, 23,* 6884–6893. [PubMed] [Article]

Zhang, X., Park, J. C., Salant, J., Thomas, S., Hirsch, J., & Hood, D. C. (2008). A multiplicative model for spatial interaction in the human visual cortex. *Journal of Vision, 8*(8):4, 1–9, http://journalofvision.org/8/8/4/, doi:10.1167/8.8.4. [PubMed] [Article]

Zlatkova, M. B., Anderson, R. S., & Ennis, F. A. (2001). Binocular summation for grating detection and resolution in foveal and peripheral vision. *Vision Research, 41,* 3093–3100. [PubMed]

Zoccolan, D., Cox, D. D., & DiCarlo, J. J. (2005). Multiple object response normalization in monkey inferotemporal cortex. *Journal of Neuroscience, 25,* 8150–8164. [PubMed] [Article]